Continuously Updated Forecasting of SARS-CoV-2 in a Regional Health System

Tori J. Finch, MS; Alexander Crowell, MS; Mamta Bhatia, MS; Jose Martinez, BS; Kadin Caines, MPH; Fei Teng, MS; Eric Watson, BS; and Michael Horberg, MD, MAS

ABSTRACT

OBJECTIVES: To build a model of local hospital utilization resulting from SARS-CoV-2 and to continuously update it with new data.

STUDY DESIGN: Retrospective analysis of real performance resulting from a model deployed in a major regional health system.

METHODS: Using hospitalization data from the Kaiser Permanente Mid-Atlantic States integrated care system during the period from March 10, 2020, through December 31, 2020, and a custom-developed genetic particle filtering algorithm, we modeled the SARS-CoV-2 outbreak in the mid-Atlantic region. This model produced weekly forecasts of COVID-19–related hospital admissions, which we then compared with actual hospital admissions over the same period.

RESULTS: We found that the model was able to accurately capture the data-generating process (weekly mean absolute percentage error, 10.0%-48.8%; Anderson-Darling *P* value of .97 when comparing percentiles of observed admissions with the uniform distribution) once the effects of social distancing could be accurately measured in mid-April. We also found that our estimates of key parameters, including the reproductive rate, were consistent with consensus literature estimates.

CONCLUSIONS: The genetic particle filtering algorithm that we have proposed is effective at modeling hospitalizations due to SARS-CoV-2. The methods used by our model can be reproduced by any major health care system for the purposes of resource planning, staffing, and population care management to create an effective forecasting regimen at scale.

Am J Manag Care. 2022;28(3):124-130. doi:10.37765/ajmc.2022.88838

Global health systems have been severely taxed by the onset of COVID-19, the disease caused by SARS-CoV-2. The disease has forced health care management organizations to adapt and obtain new capabilities that had been considered outside the typical domain of the health care management space.[1] One of the most critical requirements for health care providers has been the ability to independently forecast the impact of the outbreak on an organization's resources. To create plans around resource allocation and utilization, the Kaiser Permanente Mid-Atlantic States (KPMAS) health system required accurate models of how the disease might spread within our community and how this would affect our hospital utilization. During the epidemic, a wide variety of models intended for forecasting demand have been produced. These models span a range of structures and fitting methodologies.[2-9] We chose to employ a compartment modeling approach because of its ease of use, conceptual simplicity, proven effectiveness, and ability to flexibly specify complex models. Compartment models treat an epidemic as a system of differential equations in which patients move between discrete states. Compartment models require fitting algorithms to optimize the parameters used in their simulation forecasts. Particle filtering is one option to perform this training, with the significant advantage that this method can be trained online. Particle filtering has been used successfully in several epidemiological applications, including models of SARS-CoV-2.[10]

When translating an epidemic forecast into operational decision-making, it is critical to determine both the data inputs and outputs of the model. Many data inputs have been used for modeling the pandemic so far. Most modeling inputs include positive COVID-19 tests; unfortunately, testing volume can be strongly affected by regulatory changes in testing protocols and testing priorities.[8,9] KPMAS has experienced several significant changes to its testing policies in response to policy directives, test availability, and patient demand. These changes caused significant inconsistencies, which made testing an unreliable data source for modeling. Another popular alternative is COVID-19 deaths, because death data are less likely to undergo significant changes in data acquisition or record keeping; however, deaths are less frequent and data capture

is significantly delayed. Ultimately, hospital admissions proved to be the most effective data input for our model because hospitalization rate was a robust indicator on which to base a modeling strategy.

Using a custom package that fits compartment models on hospital admissions with a genetic particle filter, we have applied a reliable short-term forecasting framework that is currently used in KPMAS to assess and plan for the organization's immediate needs.[11] The primary output of this forecasting methodology—hospital admissions—has been used to plan an effective response for resource and personnel management across the region. Our objectives were to create a simple framework for constructing short-term forecasts of SARS-CoV-2 hospital admissions, give a realistic view into the real-time results that can be obtained by this framework, and provide a detailed comparison of this model's parameter estimates compared with the best estimates available in other literature sources.

TAKEAWAY POINTS

- We constructed a model of COVID-19 hospitalizations using a genetic particle filter to fit a modified Susceptible-Exposed-Infectious-Removed compartment model.
- After 3 weeks of warm-up, our model reliably modeled the data-generating process leading to daily hospital admissions.
- Samples of posterior distributions for key parameters and derived statistics, including attack rate, agreed with consensus estimates of these values.
- Results from this model were used in real time to make decisions about resource allocation in a major regional health system.

METHODS

Setting

Kaiser Permanente is the largest not-for-profit integrated health system in the United States, serving 12.4 million members nationwide and more than 770,000 members in the Mid-Atlantic region, representing Southern Maryland, the District of Columbia, and Northern Virginia.[12] KPMAS members are a racially and socioeconomically diverse population. The mean age of members is 47.7 years, and 27.0% of members were 60 years or older as of March 1, 2020. A total of 53.9% of members were female.

Data

We included all members of the KPMAS health care system who had active membership as of February 7, 2020. We limited our analysis to adult members, defined in our analysis as having a birth date before March 1, 2002. This provided a total population of 613,268 patients. We rounded this number to 615,000 for population modeling purposes, which constituted a change of 0.3% in the assumed population size.

When constructing our models, our primary fitting criterion was admission to a hospital with a COVID-19 diagnosis. To facilitate modeling, we extracted daily hospital admissions data for each day from March 10, 2020, through December 31, 2020. When identifying hospital admissions for modeling, we considered only the first hospital admission experienced by each patient; we did not consider readmissions as part of our daily admission counts. There is significant complexity when considering questions of readmissions, as including them would require the creation of several new compartments. This study was ruled exempt by the KPMAS Institutional Review Board.

Model Definition and Fitting

We employed an extension to the Susceptible-Exposed-Infectious-Removed, or SEIR, framework that employed explicit compartments for hospitalization and quarantine. These compartments enabled us to fit the model using hospital admissions data with a long lag between infection and hospitalization. We fit our models using a custom implementation of a genetic particle filter. We fit our model each week starting on March 31 and concluding on December 22, 2020 (the last date on which we would have a full week of validation data). Please refer to **Table 1**, which displays our selected prior distributions and compartment definitions. We offer a more detailed explanation of our model definition and fitting process in the **eAppendix** (available at **ajmc.com**).

Analytical Methods

We employed several metrics to assess model quality. We first compared the model's predictions of cumulative hospital admissions over the forecast period with the observed admissions over the period and calculated the mean absolute percentage error (MAPE) over each of the individual forecast particles. In addition to calculating the MAPE, we considered a percentile-percentile plot of the percentiles of daily hospital admissions with reference to their forecast distributions. We also examined several other statistics, particularly the attack rate and parameter values estimated by our model. For each of these statistics, we examined the posterior distribution obtained by the fitting method by extracting all values of the given parameter from particles active by the end of our fitting period. We computed our model's attack rate as the percentage of the population in any compartment other than susceptible (ie, all members who had ever been exposed). We computed the model's effective reproductive rate (R_{eff}) as the product of the contact rate (β), the inverse of the period of Infectiousness ($1/\gamma$), and the Susceptible rate (S/N).

RESULTS

Hospital Admissions

During the period from March 10, 2020, through December 31, 2020, we observed a cumulative 4301 hospital admissions for SARS-CoV-2. Of these patients, 48.9% were female. The mean age of this group was 61.8 years, and 56.8% of patients admitted to the hospital for SARS-CoV-2 were 60 years or older at the time of the admission.

METHODS

TABLE 1. Extended SEIR Model Definitions[a]

Parameter/ compartment	Description	Prior distribution/formula
Susceptible	The population of patients who may get the disease	–
Exposed	The population of patients exposed to the virus who are not yet infectious or symptomatic	–
Infectious	The population of patients who are actively spreading the virus; may be symptomatic	–
Quarantined	The population of patients who are quarantined; such patients may be physically infectious, but they are not actively mixing with the population. May be hospitalized at a later point	–
Hospitalized	The population of patients who are hospitalized and will not require a ventilator	–
Removed	The population of patients who have either recovered or died without hospitalization	–
β	The transmission coefficient of infectious patients	$\beta \sim Gamma(1.3/0.03, 0.03)$
γ	Inverse of the mean time a patient is infectious	$\gamma \sim Gamma(0.3/0.01, 0.01)$
α	Inverse of the mean period of incubation	$\alpha \sim Gamma(0.3/0.01, 0.01)$
σ	Inverse of the mean period of quarantine	$\sigma \sim Gamma(0.2/0.03, 0.03)$
h	The hospitalization rate	$h \sim Beta(9, 100)$
I(t = 0)	The starting population of the infectious compartment (mean: 5000)	$I_0 \sim 615000*\max(N(160, 20)/1000000, 100/615000)$
E(t = 0)	The starting population of the exposed compartment (mean: 5000)	$E_0 \sim 615000*\max(N(160, 20)/1000000, 100/615000)$
S(t = 0)	The starting population of the susceptible compartment (mean: 950,000)	$S_0 = 615000 - I_0 - E_0$

SEIR, Susceptible-Exposed-Infectious-Removed.

[a]Table 1 describes all compartments and parameters used in our modification to the SEIR model, along with the applicable formulae or prior distributions where applicable. Please note that all Gamma distributions used the k, θ parameterization of the Gamma distribution.

Forecast Accuracy

In the first 2 forecast periods (beginning on March 31 and April 7), the forecast significantly overestimated hospital admissions (**Figure 1**). The median estimate for cumulative hospitalizations over the 2-week forecasting period was 2.61 times larger than the true admissions in the first week and 1.86 times larger in the second. Thereafter, however, forecasts improved (Figure 1). The true observed hospital admissions were within the 99% credible interval for every week thereafter except for the weeks of June 6 and October 27, and the MAPE was consistently low (below 50% in all weeks after the first 2 forecasts) (**Table 2** and **eAppendix Figure 10**). This was especially important at the beginning of the second and third waves, which began in late June and late October, respectively. Our model was able to quickly compensate for each change (Figure 1, **Figure 2**, and **Figure 3**).

Parameter Estimates

We examined the posterior distributions observed when forecasting for the final period on December 22. We found a median incubation period of 3.2 days and a median infectious period of 3.6 days. We also estimated that patients quarantined for a mean of 8.9 days before being hospitalized and that the hospitalization rate was 5.3%, with a credible interval from 5.3% to 5.4%. Our model yielded a median attack rate estimate of 13.9%, with a 95% credible interval from 13.6% to 14.3%, by the final day of fitting on December 22, 2020.

We estimated that R_{eff} was very high (3.1) in late March; however, the introduction of social distancing measures quickly reduced this to below 1.0 by our model run on April 14. Except for the week of May 5, we estimated that R_{eff} remained below 1.0 until July. Our model estimated that R_{eff} remained above 1.0 for approximately 4 weeks in July (corresponding to the "second wave" reported in the media as social distancing guidelines were relaxed) before collapsing back below 1.0 until October. Finally, we estimated that R_{eff} was above 1.0 for each forecast date from October 20 through the end of 2020, except for the week of November 10 (which yielded an estimate of 0.96). Throughout this period, our estimate of R_{eff} varied between a median estimate of 1.04 (the final 2 forecasts of December) and 1.30 (the week of November 24).

DISCUSSION

Model Contributions and Impacts

The methodology described here can be used by health care organizations to model the continuing outbreak of SARS-CoV-2 on their own populations. Such applications would require relatively minimal technical or modeling sophistication in comparison with alternative frameworks. We believe that this model framework could be useful for any health care system that needs to model the outbreak of SARS-CoV-2 in its population.

Model Impacts to Clinical Operations

The forecasts discussed in this paper have been used extensively by KPMAS to make decisions about resource allocation around the pandemic. Initially, our forecasts were used primarily to assess burndown rates of personal protective equipment and ensure that the system rationed this equipment effectively. In addition,

clinical leadership was able to use our forecasts to determine hospital staffing needs and reschedule elective procedures when staff or bed availability was expected to run low.

Later in the pandemic, this forecast became a critical component of a secondary model that was used to forecast COVID-19–related sick leave among health care staff. These data were used in turn to plan allowable planned paid time off, overstaff in anticipation of callouts, and seek contract employees to fill predictable gaps as staff ran short.

Model Performance Over Time

Generally, after the first 2 weeks, our model fit well. However, our model failed to accurately model observed hospital admissions during our first 2 weeks of forecasts. These forecasts employ values for the contact rate (β) that are based on the first 2 weeks of modeling. These weeks predated strong local social distancing measures; thus, the primary basis for our estimate of the reproductive rate did not sufficiently account for social distancing.[13-16]

FIGURE 1. Weekly Forecast of Cumulative Hospital Admissions, April 2020[a]

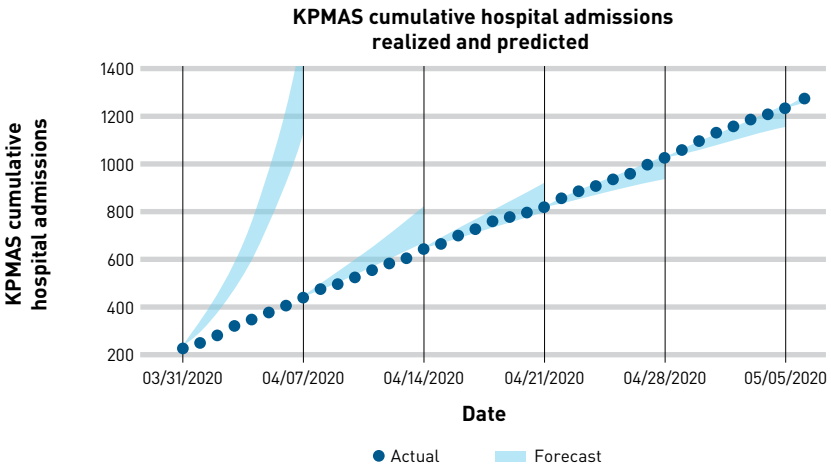

KPMAS, Kaiser Permanente Mid-Atlantic States.

[a]Figure 1 displays the actual (dark blue) and forecast 95% credible interval (light blue) of cumulative hospital admissions for the month of April 2020. Note that forecasts for the first 2 weeks predicted significantly more hospital admissions than were realized; however, the forecast quality increased significantly by the third week.

This highlights a general risk for any backward-looking modeling framework. These models assume that future system dynamics are consistent with the most recent trends in the system, which may not be true. In this case, our model failed to account for the introduction of strict social distancing measures and nonpharmaceutical interventions, including school closures and restrictions on public gatherings, dining, and more.[14-16] We observed similar results in our forecasts at the beginning of the second wave in late June and of the third wave in October.

In each of these cases, we noticed that our forecasts tended to equalize within 1 to 2 weeks of obtaining data under the new conditions. Our forecasts on June 30, 2020, underestimated hospitalizations by 48.8%; however, our forecasts were much better the following week, when we obtained a MAPE of only 23.0% (Figure 2). Our results in the third wave mirrored this trend, when we obtained a MAPE of 47.1% in the week following October 27, but this dropped to only 14.5% in the week following November 3, 2020 (Figure 3).

Overall, once the system reached an approximate steady state in mid-April, our forecasts were predictive (Figures 1 through 3, Table 2, and **eAppendix Figures 11 through 19**).

Holiday Effects on Model Performance

We can also examine the effects of holidays on the quality of our forecasts. For this analysis, we take the holidays, as recognized by the US federal government, of Memorial Day (May 25, 2020), Independence Day (July 4, 2020), Labor Day (September 7, 2020), Columbus Day (October 12, 2020), Veterans Day (November 11, 2020), Thanksgiving Day (November 26, 2020), and Christmas Day (December 25, 2020). Our forecast did not consistently over- or underestimate hospital admissions during the weeks in which each of these federal holidays occurred (Table 2). Three of these weeks were overestimated by the model, and 4 were underestimated.

Parameter Estimates

In addition to producing high-quality forecasts, our model produced a set of posterior distributions for a variety of parameters of interest. These distributions agreed well with the prevailing literature in almost all cases, although our initial value of R_{eff} (active during the first week of training) may have been too large.[17-25] This is likely because the system was underdetermined early in the fitting process. Despite this, it should be noted that estimates of the fully uncontrolled R_{eff} vary widely, and our value was well below estimates for regions like New York City.[26,27]

Our values for the controlled (with social distancing) reproductive rate, however, were far closer to the literature consensus.[19,20,23] After our forecast dated April 7, we found that this rate varied by week. Generally, we found that the rate remained within bounds of approximately 0.7 and 1.0 during periods of extended retraction, but it surged into the 1.0 to 1.3 range during the second and third waves (Table 2). In comparison, other researchers estimated state-level reproductive rates to be approximately 1.2 (1.1-1.3) during the second wave in early July.[17]

When examining the clinical meaning of compartment models, we acknowledge that there is no strict, one-to-one adherence between the compartments with clinical values. With this caveat in mind, it is informative to examine how our estimates compare with clinical

TABLE 2. Error Rates for Weekly Cumulative Hospital Admissions[a]

Forecasting weeks	MAPE over all forecasts (%)	Percentile of observed hospitalizations in forecast distribution (%)
March 31-April 6, 2020	374.6	N/A[b]
April 7-April 13, 2020	64.1	N/A[b]
April 14-April 20, 2020	15.7	25.6
April 21-April 27, 2020	19.5	94.3
April 28-May 4, 2020	21.7	96.1
May 5-May 11, 2020	27.1	2.4
May 12-May 18, 2020	11.8	31.4
May 19-May 25, 2020	16.1	11.5
May 26-June 1, 2020	37.2	6.3
June 2-June 8, 2020	13.2	72.6
June 9-June 15, 2020	12.7	43.1
June 16-June 22, 2020	39.1	5.2
June 23-June 29, 2020	16.6	43.4
June 30-July 6, 2020	48.8	99.9
July 7-July 13, 2020	23.0	41.6
July 14-July 20, 2020	21.3	71.9
July 21-July 27, 2020	22.6	69.9
July 28-August 3, 2020	33.9	11.1
August 4-August 10, 2020	24.7	36.2
August 11-August 17, 2020	17.8	31.7
August 18-August 24, 2020	16.9	63.8
August 25-August 31, 2020	15.0	45.2
September 1-September 7, 2020	20.0	78.6
September 8-September 14, 2020	28.0	39.3
September 15-September 21, 2020	22.3	59.2
September 22-September 28, 2020	15.1	66.1
September 29-October 5, 2020	47.1	19.7
October 6-October 12, 2020	35.6	98.0
October 13-October 19, 2020	27.7	84.3
October 20-October 26, 2020	16.1	76.9
October 27-November 2, 2020	47.1	8.3
November 3-November 9, 2020	14.5	59.2
November 10-November 16, 2020	41.0	99.9
November 17-November 23, 2020	17.8	65.6
November 24-November 30, 2020	21.7	11.8
December 1-December 7, 2020	15.3	60.2
December 8-December 14, 2020	11.1	33.9
December 15-December 21, 2020	10.0	48.0
December 22-December 28, 2020	17.6	14.5

MAPE, mean absolute percentage error; N/A, not applicable.

[a]Table 2 demonstrates the forecasting accuracy of our model on cumulative weekly hospital admissions. For each week, we measured the MAPE over all forecast simulations and the percentile of the observed hospitalizations within the distribution of forecast simulations. The dates for each week refer to the period over which data were collected for the comparison. Each forecast was generated at the beginning of the relevant forecast period. From these data, it is apparent that there was significant improvement in model performance after the first 2 weeks.

[b]Could not be computed because all forecasts were overestimates.

values derived from the literature. Observation of individuals has indicated that the typical period between exposure and symptom onset is approximately 6.4 days.[28] Furthermore, individuals may begin viral shedding for 1 to 3 days prior to becoming symptomatic, and viral load appears to peak within the first week of symptoms.[29-31] In comparison, our model indicated that exposed individuals may take a mean of 3.2 days to become infectious, and they may remain infectious for a mean of 3.6 days.

We estimated the period between self-quarantine and hospitalization to be approximately 8.6 days on average. This value has been estimated by various other studies to be anywhere from 5.0 days to 11.0 days.[25,32,33] Also, other studies, including randomized controlled trials of patients with COVID-19 that began tracking shortly after infection, found a variety of hospitalization rates from 3.2% to 7.1% in their control groups.[34-37] Our own estimate of 5.3% was largely consistent with these other estimates.

One outcome of great interest is the current attack rate of the virus, which is often detected using serology or antibody testing. Although there were few publicly available seroprevalence studies dating from the end of 2020 at the time of this writing, Bajema et al estimated seroprevalence of COVID-19 in Maryland at approximately 10.2%, in the District of Columbia at 6.5%, and in Virginia at 3.2% using samples taken from September 7 through September 24, 2020.[38] When weighted by the membership distribution in each jurisdiction, this indicates a serological estimate of 7.5%, although KPMAS's Virginia membership is primarily concentrated in Northern Virginia (and may therefore be underestimated by this measure). Our model forecast dated September 15, 2020, estimated an attack rate of 9.1%, with a 95% credible interval of 8.7% to 9.4%. We feel that this indicates broad agreement between the 2 measures, because subsequent studies have found that seroprevalence was significantly higher in Northern Virginia than in the state overall and because seroprevalence can underestimate overall attack rate because of rapid decay in antibody rates.[39-41]

Limitations

The chief limitation to the system that we have proposed is its reliance upon historical data and the inability to incorporate real-time information to update its R_{eff}. In practice, we demonstrated that the model may take up to 3 weeks to incorporate such changes into its forecasts.

We suggest that any organization using this model incorporate institutional and real-world knowledge into the forecasting framework provided. To do this, such organizations need only add new transitions in the system contact rate at relevant times. For instance, we might add a break point within the last 3 weeks of fitting if the local region had reopened schools or relaxed social distancing measures. This limitation, although important, is universal to any retrospective model and should be considered as a limitation upon data-based forecasting efforts in general.

The models described in this study are also limited by the data available to us. We have employed only the membership of the

KPMAS health care system for modeling. We assume that our population is representative of the mid-Atlantic region.

Conversely, our model assumes that the entire KPMAS membership is part of a single population for modeling purposes, which implies perfect social mixing. This assumption is not true because the members are spread over a wide geographic region. However, we did see that the model was able to effectively overcome this limitation. Our early (unpublished) experiments on subpopulations indicated that there was no forecasting accuracy to be gained by modeling these groups individually. In general, we strongly recommend that any users attempting to use this framework on a diverse population investigate whether the framework is more effective when applied to each subpopulation.

CONCLUSIONS

Using a genetic particle filtering methodology, we constructed a weekly rolling forecast of hospital admissions. When conditions remained stable, we found that this methodology produced highly accurate forecasts of hospital admissions. Furthermore, our model produced convincing posterior distributions of several key variables of interest in the COVID-19 literature.

Beyond the contributions of this study's specific methodology to the health care management domain, we also have demonstrated the effectiveness of a new extension to the particle filter fitting technique—genetic particle filtering—on real data. To our knowledge, this constitutes the first use of this technique in a real-life epidemiological setting. When combined with our strong performance results, we believe that the advantages of this methodology (conceptual simplicity and computational efficiency) imply that it should be explored further in the epidemiological literature. ■

FIGURE 2. Weekly Forecast of Cumulative Hospital Admissions, July 2020[a]

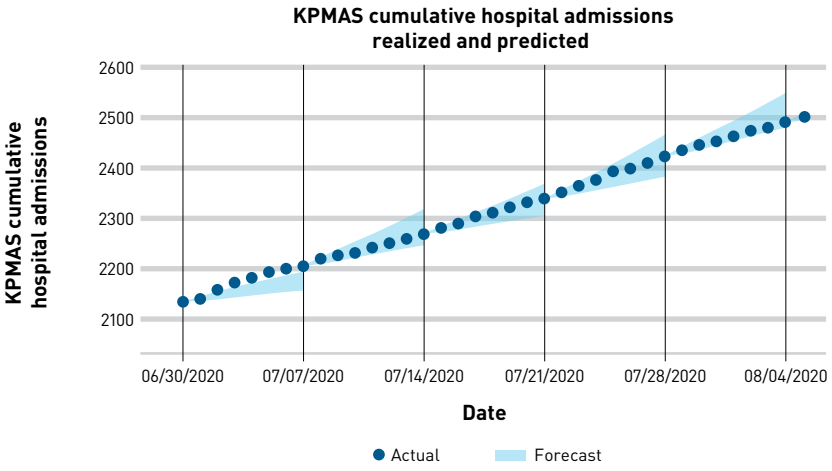

KPMAS, Kaiser Permanente Mid-Atlantic States.

[a]Figure 2 displays the actual (dark blue) and forecast 95% credible interval (light blue) of cumulative hospital admissions for the month of July 2020. Hospital admissions experienced a significant and unexpected uptick at the beginning of the month; however, the model was able to adapt quickly, and hospital admissions landed within the credible interval during future weeks.

FIGURE 3. Weekly Forecast of Cumulative Hospital Admissions, November 2020[a]

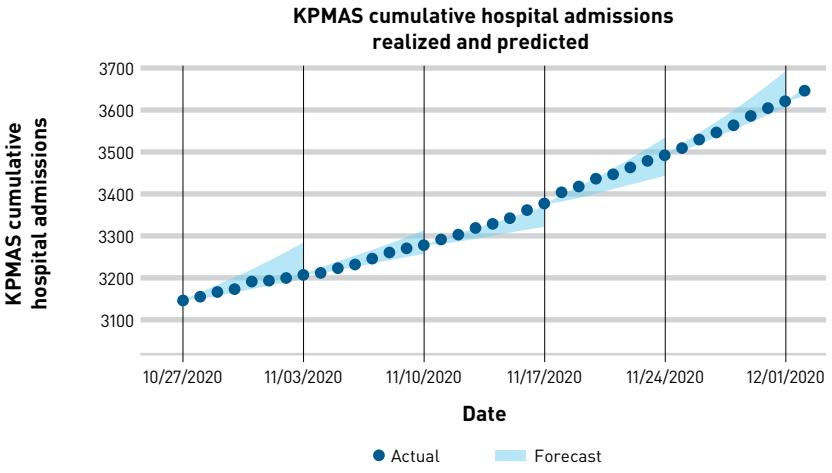

KPMAS, Kaiser Permanente Mid-Atlantic States.

[a]Figure 3 displays the actual (dark blue) and forecast 95% credible interval (light blue) of cumulative hospital admissions for the month of November 2020. This figure captures the most significant uptick in hospital admissions during the winter 2020 surge. Weekly forecasts displayed some uncertainty as to the magnitude of the surge, but realized admissions remained within expected bounds overall.

Author Affiliations: Kaiser Permanente Mid-Atlantic Permanente Medical Group (TJF, AC, MB, JM, FT, EW, MH), Rockville, MD; Kaiser Permanente Mid-Atlantic Permanente Research Institute (MB, EW, MH), Rockville, MD; Kaiser Foundation Health Plan of the Mid-Atlantic States (KC), Rockville, MD.

Source of Funding: This research is funded by the Mid-Atlantic Permanente Medical Group and the Kaiser Permanente Mid-Atlantic States Community Health Program.

Author Disclosures: Mr Teng is employed as a data analyst by the Mid-Atlantic Permanente Medical Group and received SARS-CoV-2 data from the Mid-Atlantic Permanente Medical Group data system. The authors report no relationship or financial interest with any entity that would pose a conflict of interest with the subject matter of this article.

Authorship Information: Concept and design (TJF, AC, MB, JM, MH); acquisition of data (TJF, KC, FT, MH); analysis and interpretation of data (TJF, AC, KC, FT, MH); drafting of the manuscript (TJF, AC, EW); critical revision of the manuscript for important intellectual content (TJF, AC, MB, JM, EW, MH); statistical analysis (TJF, AC); administrative, technical, or logistic support (MB, KC, FT, EW, MH); and supervision (TJF, JM, MH).

Address Correspondence to: Tori J. Finch, MS, Kaiser Permanente Mid-Atlantic Permanente Medical Group, 2101 E Jefferson St, Rockville, MD 20852. Email: Tori.J.Finch@kp.org.

REFERENCES

1. Slotkin JR, Murphy K, Ryu J. How one health system is transforming in response to COVID-19. *Harvard Business Review*. June 11, 2020. Accessed February 3, 2022. https://hbr.org/2020/06/how-one-health-system-is-transforming-in-response-to-covid-19
2. COVID-19 policy briefings. Institute for Health Metrics and Evaluation. Accessed September 14, 2020. http://www.healthdata.org/covid/updates
3. Borchering RK, Viboud C, Howerton E, et al. Modeling of future COVID-19 cases, hospitalizations, and deaths, by vaccination rates and nonpharmaceutical intervention scenarios – United States, April-September 2021. *MMWR Morb Mortal Wkly Rep*. 2021;70(19):719-724. doi:10.15585/mmwr.mm7019e3
4. COVID-19: what's new for May 4, 2020. Institute for Health Metrics and Evaluation. May 2020. Accessed September 14, 2020. http://www.healthdata.org/sites/default/files/files/Projects/COVID/Estimation_update_050420.pdf
5. COVIDScenarioPipeline. GitHub. March 2020. Accessed September 14, 2020. https://github.com/HopkinsIDD/COVIDScenarioPipeline
6. DELPHI: the epidemiological model underlying COVID analytics. GitHub. May 2020. Accessed September 14, 2020. https://github.com/COVIDAnalytics/DELPHI/graphs/code-frequency
7. Zou D, Wang L, Xu P, Chen J, Zhang W, Gu Q. Epidemic model guided machine learning for COVID-19 forecasts in the United States. *medRxiv*. Preprint posted online May 25, 2020. doi:10.1101/2020.05.24.20111989
8. Bayesian compartmental models for COVID-19. GitHub. April 2020. Accessed September 14, 2020. https://github.com/dsheldon/covid
9. COVID-19 projection in the US. GitHub. April 2020. Accessed September 14, 2020. https://github.com/shaman-lab/COVID-19Projection
10. Romero-Severson EO, Hengartner N, Meadors G, Ke R. Change in global transmission rates of COVID-19 through May 6 2020. *PLoS One*. 2020;15(8):e0236776. doi:10.1371/journal.pone.0236776
11. Fast facts. Kaiser Permanente. Accessed September 14, 2020. https://about.kaiserpermanente.org/who-we-are/fast-facts
12. Hespanhol L, Vallio CS, Costa LM, Saragiotto BT. Understanding and interpreting confidence and credible intervals around effect estimates. *Braz J Phys Ther.* 2019;23(4):290-301. doi:10.1016/j.bjpt.2018.12.006
13. Governor Hogan announces closure of all non-essential businesses, $175 million relief package for workers and small businesses affected by COVID-19. News release. The Office of Governor Larry Hogan; March 23, 2020. Accessed September 14, 2020. https://governor.maryland.gov/2020/03/23/governor-hogan-announces-closure-of-all-non-essential-businesses-175-million-relief-package-for-workers-and-small-businesses-affected-by-covid-19/
14. COVID-19 surveillance. Government of the District of Columbia. Accessed February 3, 2022. https://coronavirus.dc.gov/data
15. COVID-19 data in Virginia. Virginia Department of Health. Accessed February 3, 2022. https://www.vdh.virginia.gov/coronavirus/see-the-numbers/covid-19-in-virginia/
16. Ferguson N, Laydon D, Nedjati-Gilani G, et al. Report 9: impact of non-pharmaceutical interventions (NPIs) to reduce COVID19 mortality and healthcare demand. Imperial College London. March 16, 2020. Accessed February 3, 2022. https://spiral.imperial.ac.uk/bitstream/10044/1/77482/14/2020-03-16-COVID19-Report-9.pdf
17. Abbott S, Hellewell J, Thompson R, et al. Temporal variation in transmission during the COVID-19 outbreak. epiforecasts.io. Accessed February 3, 2022. https://epiforecasts.io/covid/
18. Abbott S, Munday JD, Hellewell J, et al. Temporal variation in transmission during the COVID-19 outbreak in Italy. Centre for Mathematical Modelling of Infectious Diseases. March 19, 2020. Accessed September 14, 2020. https://cmmid.github.io/topics/covid19/reports/national-time-varying-transmission/italy.pdf
19. Hellewell J, Abbott S, Gimma A, et al; Centre for the Mathematical Modelling of Infectious Diseases COVID-19 Working Group. Feasibility of controlling COVID-19 outbreaks by isolation of cases and contacts. *Lancet Glob Health*. 2020;8(4):e488-e496. doi:10.1016/S2214-109X(20)30074-7
20. Lauer SA, Grantz KH, Bi Q, et al. The incubation period of coronavirus disease 2019 (COVID-19) from publicly reported confirmed cases: estimation and application. *Ann Intern Med*. 2020;172(9):577-582. doi:10.7326/M20-0504
21. Li R, Pei S, Chen B, et al. Substantial undocumented infection facilitates the rapid dissemination of novel coronavirus (SARS-CoV-2). *Science*. 2020;368(6490):489-493. doi:10.1126/science.abb3221
22. Verity R, Okell LC, Dorigatti I, et al. Estimates of the severity of coronavirus disease 2019: a model-based analysis. *Lancet Infect Dis*. 2020;20(6):669-677. doi:10.1016/S1473-3099(20)30243-7
23. Zhang J, Litvinova M, Liang Y, et al. Age profile of susceptibility, mixing, and social distancing shape the dynamics of the novel coronavirus disease 2019 outbreak in China. *medRxiv*. Preprint posted online March 20, 2020. doi:10.1101/2020.03.19.20039107
24. Zhou F, Yu T, Du R, et al. Clinical course and risk factors for mortality of adult inpatients with COVID-19 in Wuhan, China: a retrospective cohort study. *Lancet*. 2020;395(10229):1054-1062. doi:10.1016/S0140-6736(20)30566-3
25. Liu Y, Gayle AA, Wilder-Smith A, Rocklöv J. The reproductive number of COVID-19 is higher compared to SARS coronavirus. *J Travel Med*. 2020;27(2):taaa021. doi:10.1093/jtm/taaa021
26. Ives AR, Bozzuto C. State-by-state estimates of R0 at the start of COVID-19 outbreaks in the USA. *medRxiv.* Preprint posted online May 27, 2020. doi:10.1101/2020.05.17.20104653
27. Epiforecasts COVID-19. GitHub. June 2020. Accessed September 14, 2020. https://github.com/epiforecasts/covid-us-forecasts
28. Backer JA, Klinkenberg D, Wallinga J. Incubation period of 2019 novel coronavirus (2019-nCoV) infections among travellers from Wuhan, China, 20-28 January 2020. *Euro Surveill*. 2020;25(5):2000062. doi:10.2807/1560-7917.ES.2020.25.5.2000062
29. Wei WE, Li Z, Chiew CJ, Yong SE, Toh MP, Lee VJ. Presymptomatic transmission of SARS-CoV-2 — Singapore, January 23–March 16, 2020. *MMWR Morb Mortal Wkly Rep*. 2020;69(14):411-415. doi:10.15585/mmwr.mm6914e1
30. Pan Y, Zhang D, Yang P, Poon LLM, Wang Q. Viral load of SARS-CoV-2 in clinical samples. *Lancet Infect Dis*. 2020;20(4):411-412. doi:10.1016/S1473-3099(20)30113-4
31. Tindale LC, Stockdale JE, Coombe M, et al. Evidence for transmission of COVID-19 prior to symptom onset. *eLife*. 2020;9:e57149. doi:10.7554/eLife.57149
32. Huang C, Wang Y, Li X, et al. Clinical features of patients infected with 2019 novel coronavirus in Wuhan, China. *Lancet*. 2020;395(10223):497-506. doi:10.1016/S0140-6736(20)30183-5
33. Cummings MJ, Baldwin MR, Abrams D, et al. Epidemiology, clinical course, and outcomes of critically ill adults with COVID-19 in New York City: a prospective cohort study. *Lancet*. 2020;395(10239):1763-1770. doi:10.1016/S0140-6736(20)31189-2
34. Mitjà O, Corbacho-Monné M, Ubals M, et al. Hydroxychloroquine for early treatment of adults with mild coronavirus disease 2019: a randomized, controlled trial. *Clin Infect Dis*. 2021;73(11):e4073-e4081. doi:10.1093/cid/ciaa1009
35. Skipper CP, Pastick KA, Engen NW, et al. Hydroxychloroquine in nonhospitalized adults with early COVID-19: a randomized trial. *Ann Intern Med*. 2020;173(8):623-631. doi:10.7326/M20-4207
36. Gottlieb PL, Nirula A, Chen P, et al. Effect of bamlanivimav as monotherapy or in combination with etesevimab on viral load in patients with mild to moderate COVID-19: a randomized clinical trial. *JAMA*. 2021;325(7):632-644. doi:10.1001/jama.2021.0202
37. Tardif JC, Bouabdallaoui N, L'Allier PL, et al. Efficacy of colchicine in non-hospitalized patients with COVID-19; COLCORONA Investigators. *medRxiv*. Preprint posted online January 27, 2021. doi:10.1101/2021.01.26.21250494
38. Bajema KP, Wiegand RE, Cuffe K, et al. Estimated SARS-CoV-2 seroprevalence in the US as of September 2020. *JAMA Intern Med*. 2021;181(4):450-460. doi:10.1001/jamainternmed.2020.7976
39. Rogawski McQuade ET, Guertin KA, Becker L, et al. Assessment of seroprevalence of SARS-CoV-2 and risk factors associated with COVID-19 infection among outpatients in Virginia. *JAMA Netw Open*. 2021;4(2):e2035234. doi:10.1001/jamanetworkopen.2020.35234
40. Ibarrondo FJ, Fulcher JA, Goodman-Meza D, et al. Rapid decay of anti-SARS-CoV-2 antibodies in persons with mild Covid-19. *N Engl J Med*. 2020;383(11):1085-1087. doi:10.1056/NEJMc2025179
41. Self WH, Tenforde MW, Stubblefield WB, et al; CDC COVID-19 Response Team; IVY Network. Decline in SARS-CoV-2 antibodies after mild infection among frontline health Care personnel in a multistate hospital network — 12 states, April – August 2020. *MMWR Morb Mortal Wkly Rep*. 2020;69(47):1762-1766. doi:10.15585/mmwr.mm6947a2

Visit **ajmc.com/link/88838** to download PDF and eAppendix

Supplement – Model Definition

Our forecasting methodology employed a Genetic Particle Filter (GPF), which we applied to a modified SEIR compartment model. In this supplement, we will review the construction of both the SEIR model and our GPF algorithm, along with our reasoning for using this method.

Compartment Models

Compartment models are an epidemiological tool for forward simulation of disease spread. Members of a population are assigned to a collection of compartments, each of which indicates a distinct step in an individual patient's disease course. Traditionally, these compartments are **S**usceptible (not yet infected), **E**xposed (exposed, but not yet capable of spreading the disease to others), **I**nfectious (impacted by the disease and capable of spreading it to other members of the population), and **R**emoved (no longer capable of infecting others or being infected, typically due either to death or because of acquired immunity).

This model can be used to simulate disease spread using a series of Differential Equations. Members of the population move through each compartment according to either the static governing equations or a value drawn from a generating distribution. Typically, members of the Infectious compartment have the potential to expose others, expressed by moving patients from the Susceptible compartment into the Exposed. Transition between the other compartments is governed by a static or memoryless random transition process (such as a Poisson process).

Modified SEIR Model

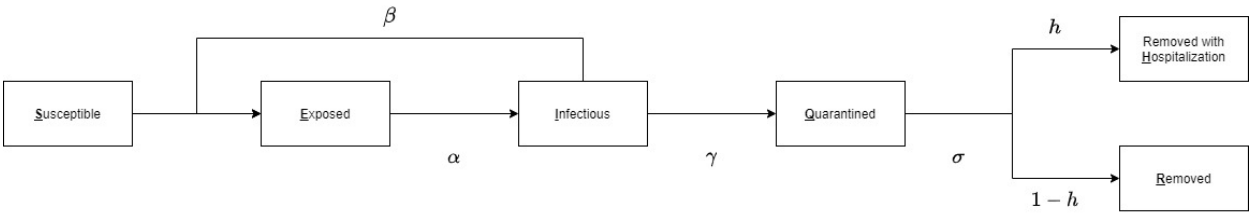

Distinct diseases may also be modeled with modified versions of this framework. One popular extension is to allow members to transition from the Infectious compartment back to the Susceptible compartment (to reflect diseases in which acquired immunity is fleeting). In our review of the literature on modeling SARS COV-2, we found that most infectious spread occurs in the pre-symptomatic stages or in the early symptomatic stages at the beginning of a patient's infection ; however, patients could frequently spend relatively long periods between becoming symptomatic and requiring a hospitalization.[1] This prompted us to incorporate an additional **Q**uarantined compartment, which would represent this period between a patient having the potential to spread the virus and hospitalization or recovery.

In addition, we also incorporated a 'split'; members of the Quarantined compartment can transition to either a **H**ospitalized compartment or to a regular Removed compartment. In our model, the Hospitalized compartment represents a patient that has been removed from the population with a hospitalization, and we do not model internal hospital dynamics. Therefore, the population of the Hospitalization compartment includes all patients that have ever been hospitalized due to SARS COV-2. We decided not to explicitly model internal hospital dynamics because these dynamics were not likely to impact the rest of the model (since hospitalized patients were strictly quarantined and infection rates in our healthcare staff were

low) and our primary output was hospital admissions. It is possible to construct a separate model of hospital, Emergent Care, and Intensive Care dynamics using a simulation that takes entrants into the Hospitalized compartment as inputs.

Please note that, in constructing the transitions from the Quarantined compartment into either the Hospitalized or Removed compartments, we employ a single transition rate (σ), along with a hospitalization rate (h). An alternative construction of this model could use two rates (σ_H and σ_R). Because we used a Poisson process to model outflows from this compartment and we split these flows according to a Binomial distribution with h as our proportion of hospitalizations, these two model descriptions are identifiable. To verify this, it is only necessary to note that the sum of two independent Poisson processes is itself a Poisson process, and the distribution of a Poisson variate conditioned upon its sum with an independent Poisson variate is Binomial.[2] Our parameterization was advantageous because we were more confident in our prior belief regarding the hospitalization rate h than we were in either of the outflow rates we could have modeled otherwise (σ_H and σ_R).

During forward simulation, we employed a Poisson process to model transitions between compartments. We chose this process as our modeling framework because the Poisson process is memoryless, meaning that we would not have to account for the time any individual member of the population spent in any given compartment. This is a generalization to the static rate incorporated by deterministic compartment models, which is also necessarily memoryless.

Genetic Particle Filter

To fit our models, we wrote a Genetic Particle Filtering algorithm in the Python programming language. The Particle Filtering (PF) approach is a Bayesian model fitting methodology that allows for online learning, which was a strong advantage for a model which would have to be run many times, incorporating slightly more data each time.

Traditional PF models incorporate a simulate-and-eliminate method of fitting. The model begins by constructing many sets of parameters and starting conditions (each called a 'particle'). Then, the model simulates each particle according to some dynamic rules for a set period (such as the stochastic numerical integration we described above). Then, each particle is evaluated by comparing its outputs with the outputs obtained by the data. If enough particles are sufficiently unlikely, the whole body of particles is resampled (with replacement) according to the relative likelihood of each model to produce the data.

Some authors incorporate slight alterations to this framework. For example, Li, et al. eliminated the resampling step to instead use a genetic algorithm. In the genetic algorithm, particles with low likelihood are altered to look more like higher-quality particles. We employed a simplified version of the algorithm described by Li, et al. wherein we omit the mutation step.[3] Our algorithm follows.

1. For n = 1 : N, do
    a. Draw an initial set of parameters

$$\rho_{0,n} \sim Prior(\rho_{0,n})$$

    b. Draw an initial set of state estimates

$$X_{0,n} \sim Prior(X_{0,n})$$

    c. Set the initial weight of each sample to an arbitrary constant ($w_{0,n} = \frac{1}{N}$).

    d. Set the initial time $t = 0$.

2. For each daily observation with date t_1 and number of hospitalizations Y_{t_1}, do

    a. For n = 1 : N do

        i. While $t < t_1$ do

            1. If a parameter resampling point has been reached, resample that parameter from its new prior.

$$\rho_{t,n} \sim Prior(\rho_{t,n})$$

            2. Forward simulate by 1 time-step (dt using stochastic system dynamics (as described above).

            3. Set $t = t + dt$

        ii. Calculate the probability of obtaining the observed number of hospitalizations from the simulated outflows from the Infected compartment and update the particle weights.

$$\widetilde{w_{t,n}} = w_{t-1,n} * (B(Y_t | H_t - H_{t-1}, h_n) + 0.0001)$$

        Where $B(Y|N,p)$ represents the Binomial Probability Mass Function (PMF) of observing Y successes, given a total population size N and success probability p.

        Note that we add a small constant offset to prevent numerical overflow errors when probabilities are vanishingly small.

        iii. Normalize weights for all samples.

$$w_{t,n} = \frac{\widetilde{w_{t,n}}}{\sum_n \widetilde{w_{t,n}}}$$

        iv. Calculate the effective sample size

$$S_{eff} = \sum_{n} \frac{1}{{w_{t,n}}^2}$$

b. If $S_{eff} < S_{min}$ do

   i. Select the top $Floor(S_{eff})$ samples by weight $w_{t,n}$; label this as set A

   ii. Select all samples that are not part of set A; label this as set B

   iii. For i in $1 : (N - Floor(S_{eff}))$ do

      1. Randomly select a particle p_A from set A uniformly

      2. Randomly select a particle p_B from set B uniformly

      3. Calculate $b = \frac{w_{p_A}}{w_{p_A} + w_{p_B}}$

      4. Create a new particle p_{new}; for each parameter or value x_{new}, set

$$x_{new} = b * x_A + (1 - b) * x_B$$

   iv. Add the new particle p_{new} to particle set C

c. Combine particle sets A and C to create a final set of particles to continue modeling

Hyperparameters and Model Fitting

We used 20,000 particles to fit our models. We used an effective sample size of 12,000 as our cut-off to genetically re-sample particles. Each week, we resampled the contact rate (β) from the prior $\Gamma(43.3,0.03)$. Because our initial experimentation demonstrated that it took approximately three weeks for the contact rate parameter to converge, we skipped the resampling step for the two weeks prior to producing each forecast.

Weekly Fitting Process

We employed a rolling fitting procedure that produced forecasts on a weekly basis. We observed our first COVID-19-related hospitalization on March 17th, 2020 and elected to begin our training period one week before that date. Based on simulations and experimenting with fitting quality, we found that it took approximately three weeks for our model to accurately capture system dynamics. Based on this information, we decided to 'freeze' the contact rate (β) three weeks prior to our forecasting date but employed weekly resampling of this parameter prior to that time. This led us to the following process:

1. Sample all parameters and starting values on March 10th, 2020 and create our first model checkpoint
2. On every 7th day (one week) until the end of the experimental period:
    a. Recover the previous model checkpoint
    b. Run particle filter daily for 7 days
    c. Create a new model checkpoint
    d. Run particle filter daily for another 14 days (brings us to the date of the forecast)
    e. Construct a forecast of the following two weeks using forward simulation with the latest parameters

We ran this process for 39 weeks, starting from March 31st, 2020 (three weeks from the beginning of our training data) through December 22nd, 2020.

Parameter Estimation

To obtain estimates for a model parameter or other outcome measure (such as attack rate), we examined the posterior distribution obtained by the fitting method by extracting all values of the

given parameter from particles active by the end of our fitting period or the indicated fitting week. We computed our model's attack rate as the percentage of the population in any compartment other than Susceptible (i.e. all members that had ever been Exposed). We computed the model's effective reproductive rate (R_{eff}) as the product of the contact rate (β), the inverse of the period of Infectiousness ($\frac{1}{\gamma}$), and the Susceptible rate ($\frac{S}{N}$).

References

1. He X, Lau EHY, Wu P, et al. Temporal dynamics in viral shedding and transmissibility of COVID-19 [published correction appears in Nat Med. 2020 Sep;26(9):1491-1493]. *Nat Med*. 2020;26(5):672-675. doi:10.1038/s41591-020-0869-5
2. Feller W. Chapter 9: *Introduction to Probability Theory and its applications, vol 1*.John Wiley. 2008
3. Li K, Wu J, Zhang Q, et al. New Particle Filter Based on GA for Equipment Remaining Useful Life Prediction. Sensors (Basel). 2017;17(4):696. doi: 10.3390/s17040696. PubMed PMID: 28350341.

Supplementary Results

eAppendix Figure 1. Weekly Hospital Admission Forecasts

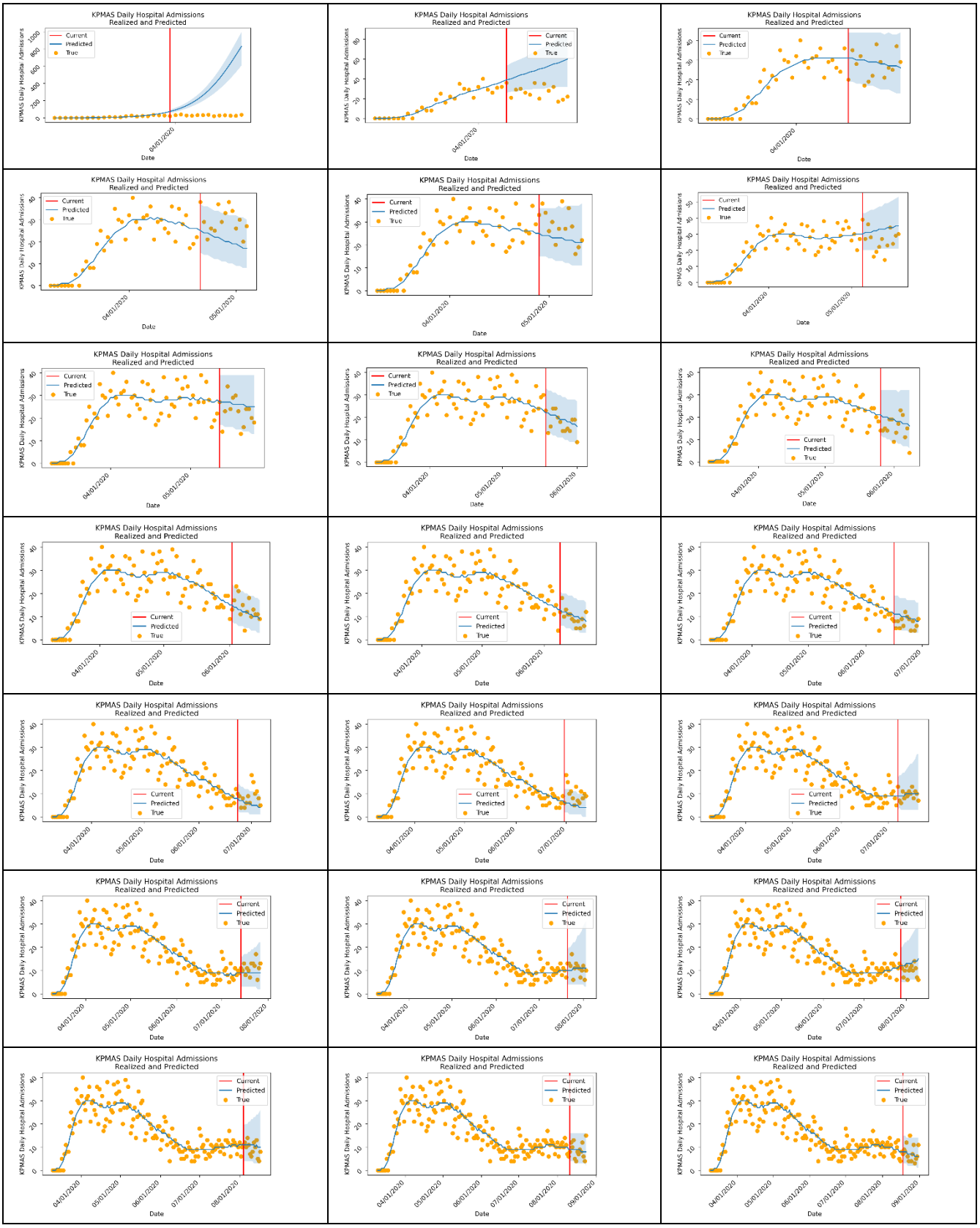
KPMAS Daily Hospital Admissions
Realized and Predicted
Current
Predicted
True
KPMAS Daily Hospital Admissions
Date

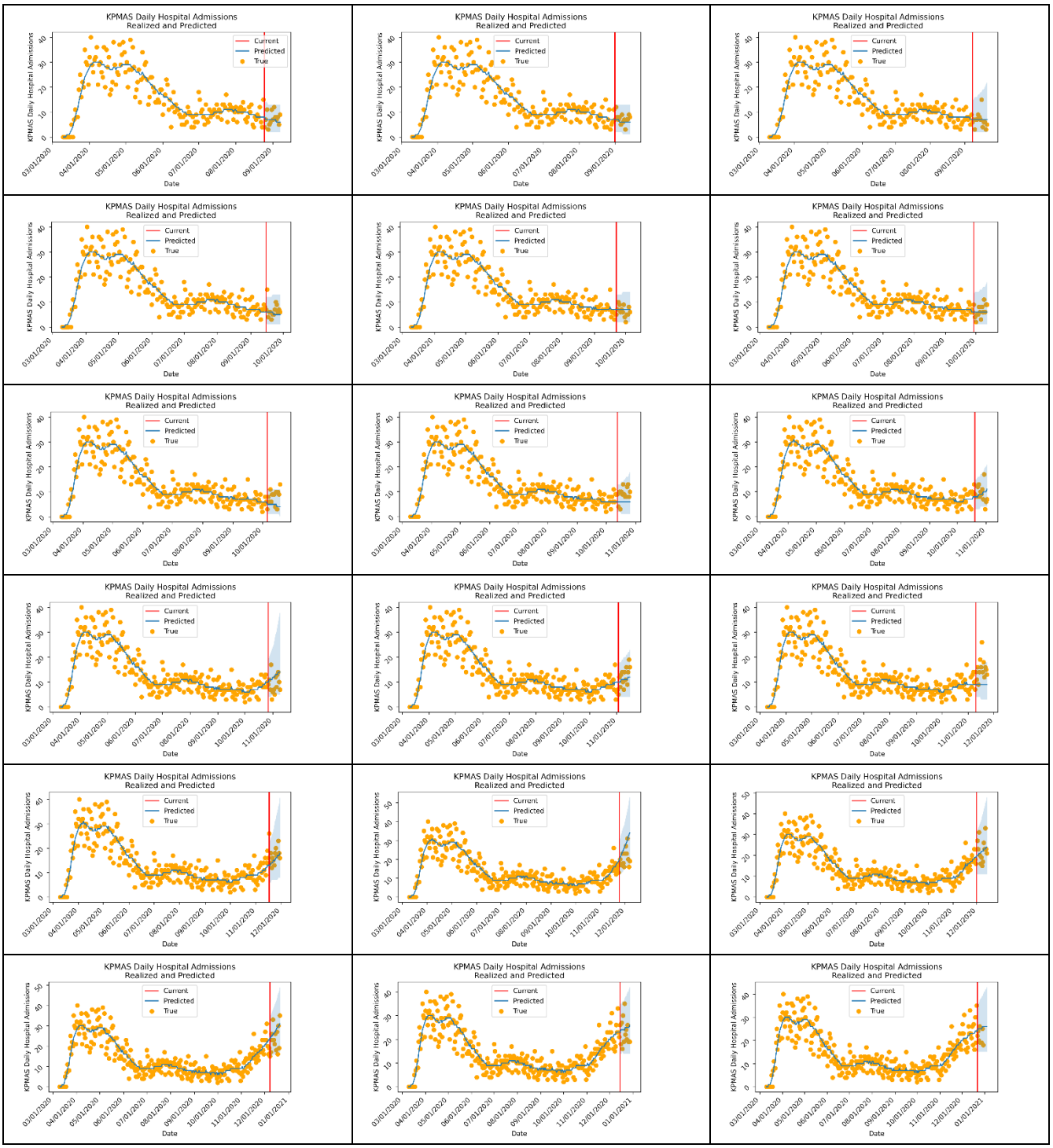

eAppendix Figure 1 displays the weekly hospital admissions (orange), along with our forecasts over the same period and the 95% Credible Interval. The red line indicates the final date of training data available for fitting.

eAppendix Figure 2. Final Posterior Distribution Estimate of Alpha

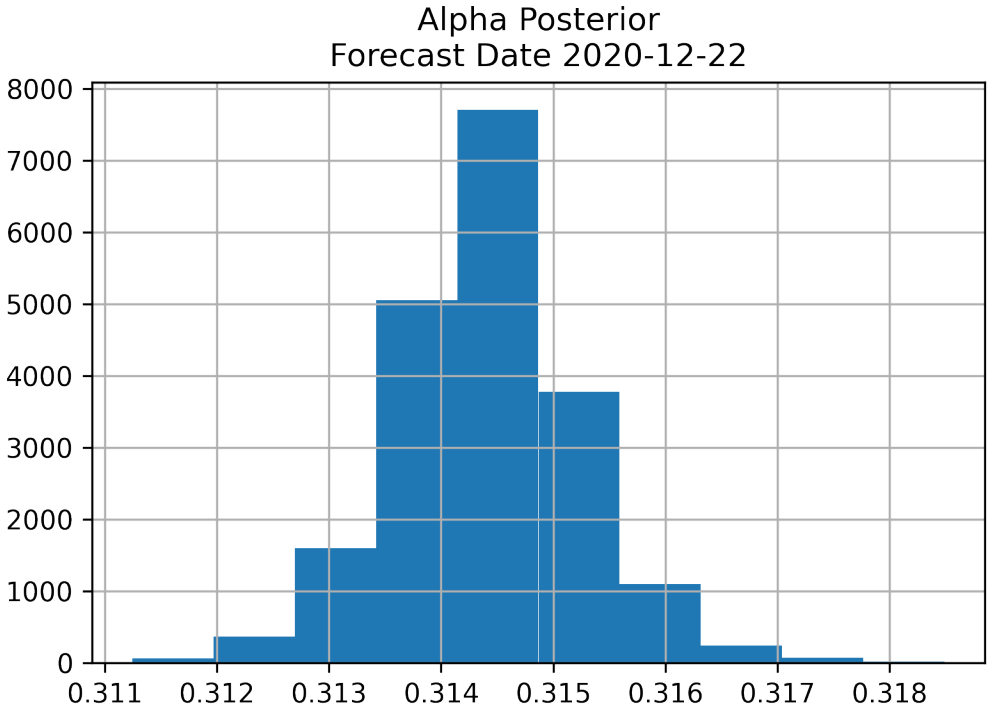

eAppendix Figure 2 displays the final posterior distribution of alpha (the inverse of the incubation period) estimated using all our fitting data. This median estimate of this parameter corresponded to an average incubation period of 3.2 days.

eAppendix Figure 3. Final Posterior Distribution Estimate of Gamma

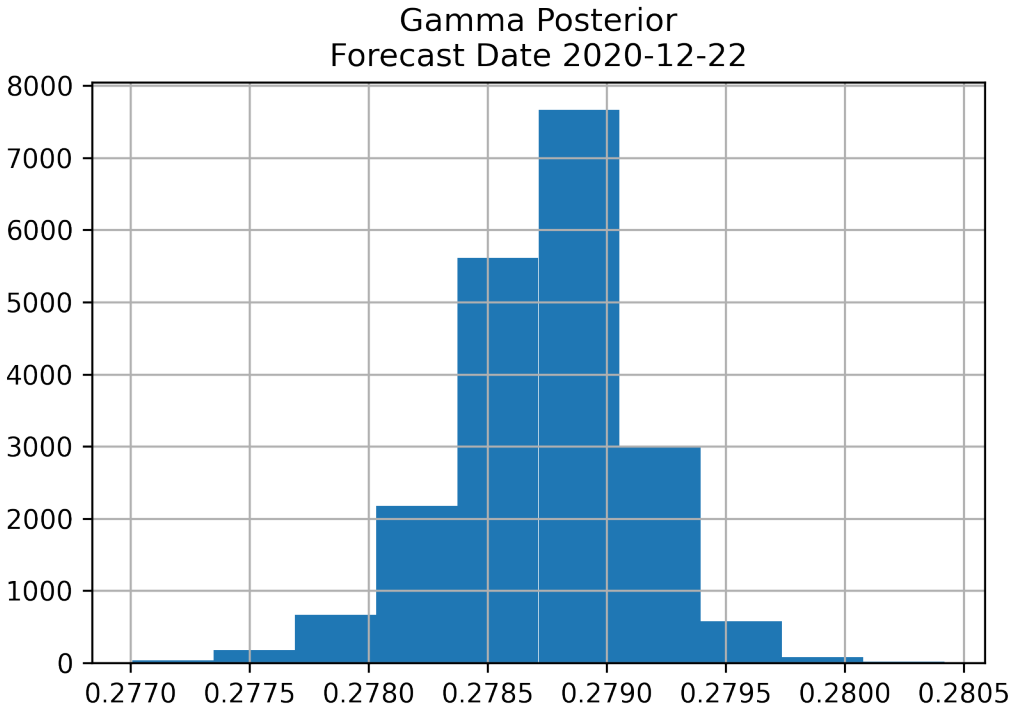

eAppendix Figure 3 displays the final posterior distribution of gamma (the inverse of the infectious period) estimated using all our fitting data. This median estimate of this parameter corresponded to an average infectious period of 3.6 days.

eAppendix Figure 4. Final Posterior Distribution Estimate of Sigma

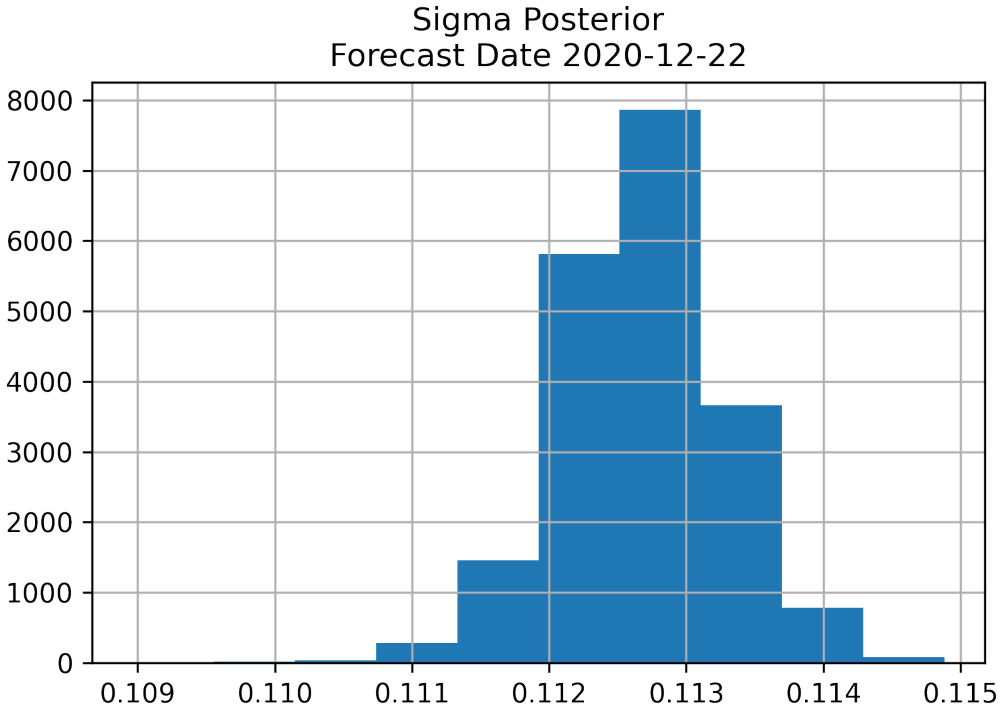

eAppendix Figure 4 displays the final posterior distribution of sigma (the inverse of the quarantine period) estimated using all our fitting data. This median estimate of this parameter corresponded to an average infectious period of 8.9 days.

eAppendix Figure 5. Final Posterior Distribution Estimate of COVID Hospitalization Rate

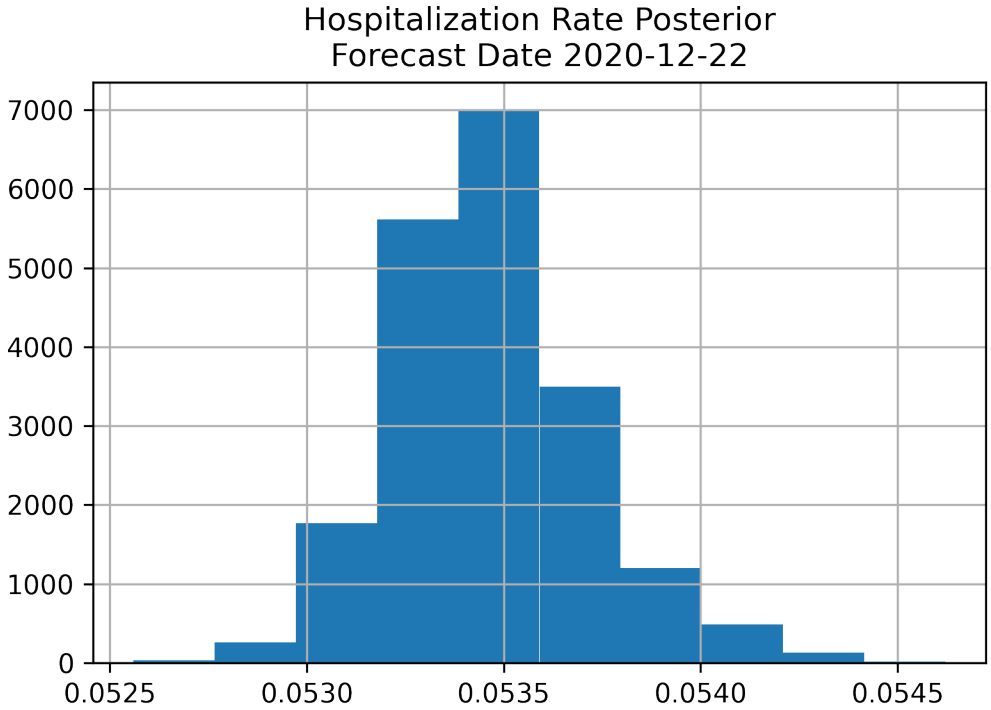

eAppendix Figure 5 displays the final posterior distribution of the hospitalization rate estimated using all our fitting data. This median estimate of this parameter corresponded to a hospitalization rate of 5.34%.

eAppendix Figure 6: Effective Reproductive Rate by Week

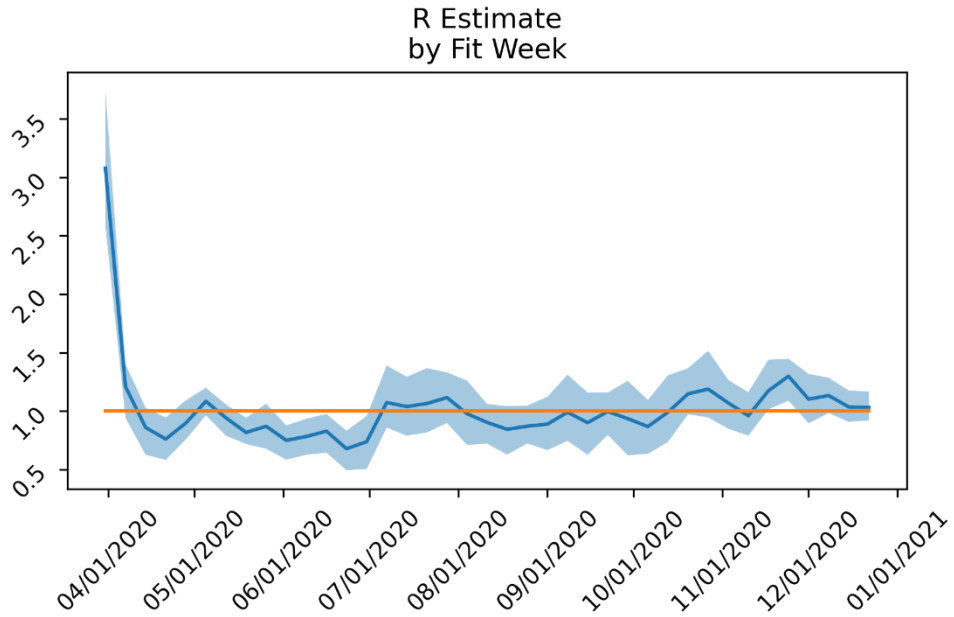

eAppendix Figure 6 displays the median estimate and 95% Credible Interval of the effective reproductive rate (R_{eff}). The posterior estimates used for this figure were taken from the active model on the given date, using all of the fitting data to that point. The reproductive rate started very high in the middle of March, but quickly decreased to approximately 1 by the middle of April. We observed two periods where the effective reproductive rate increased to above 1.0 for extended periods; in July 2020 (the 'second wave') and again in late October through the end of the year (the 'third wave').

eAppendix Figure 7. Posterior Distribution of Cumulative Attack Rate by December 22nd, 2020

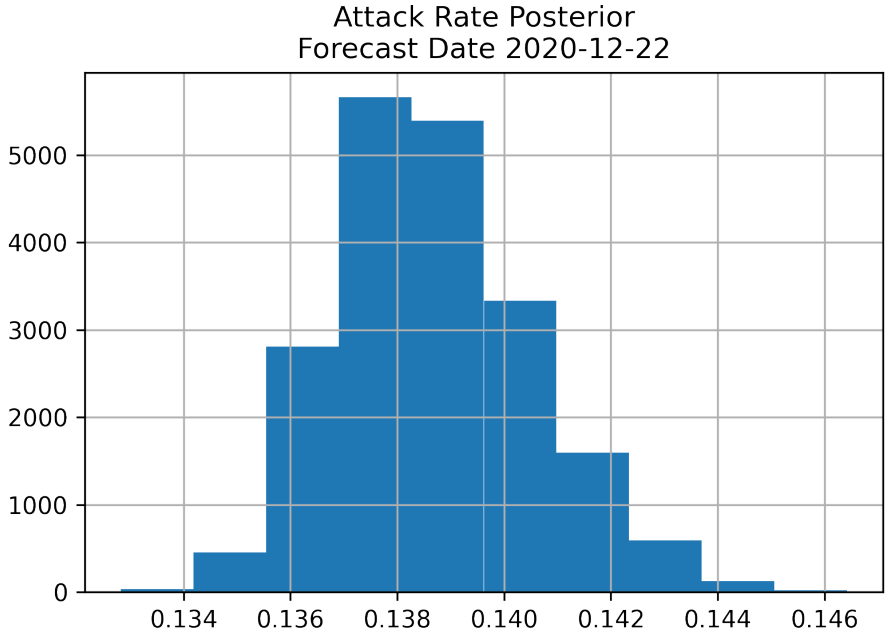

eAppendix Figure 7 posterior distribution of our cumulative attack rate by the end of the fitting period (December 22nd, 2020). The cumulative attack rate here refers to the percentage of individuals that were no longer in the Susceptible population by the relevant date. The median estimate from this distribution was 13.9%.

eAppendix Figure 8: Hospital Admissions Forecast P-P Plot

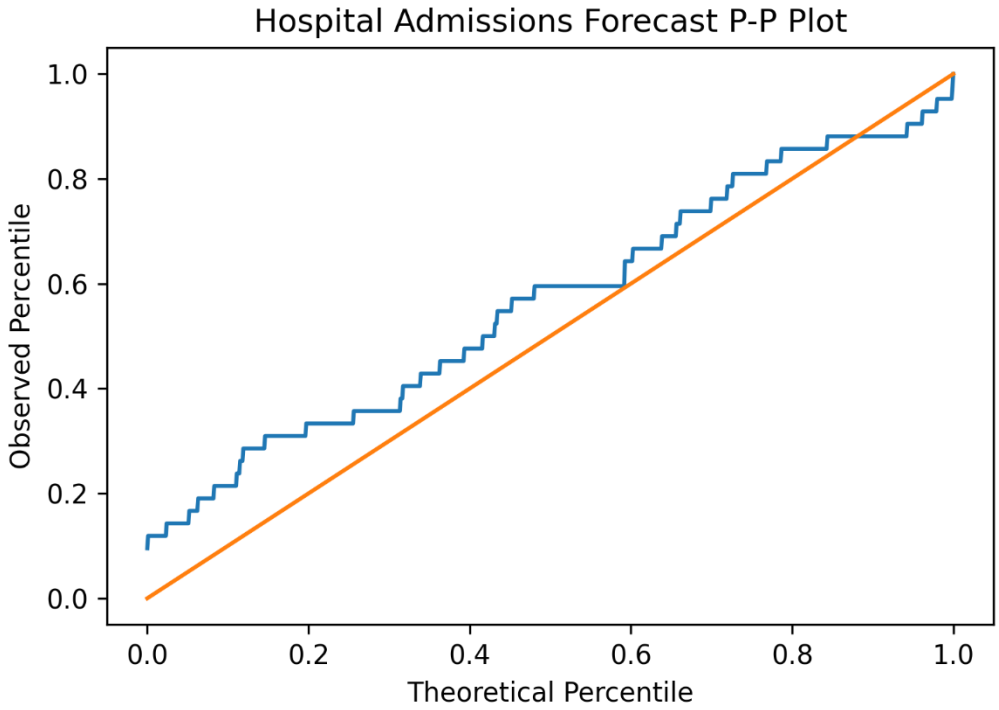

eAppendix Figure 8 displays the Percentile-Percentile (P-P) plot. We construct the observed percentiles by obtaining the percentile of each week's hospital admissions data in the bootstrap probability distribution of that same week's most recent forecast. If this distribution closely resembles the uniform distribution (the orange line), then we would say that our forecast closely resembles the generating distribution. In this case, we note that there is a concentration of observations in which the true value is a very low (or 0^{th}) percentile, indicating that our forecasts tended to overestimate future hospitalizations. This was largely attributable to the significant overestimates obtained in the first two weeks of forecasting.

eAppendix Figure 9: Hospital Admissions Forecast P-P Plot (excluding First Two Weeks)

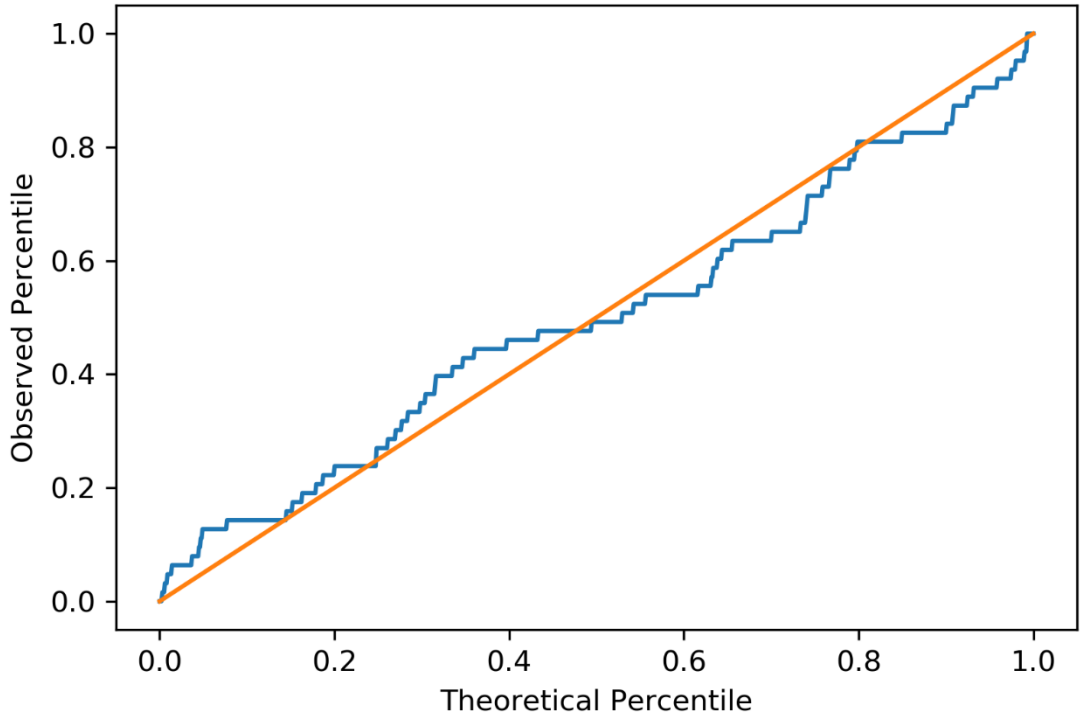

eAppendix Figure 9 displays the Percentile-Percentile (P-P) plot of weekly forecasts. We construct the observed percentiles by obtaining the percentile of each week's cumulative hospital admissions data in the bootstrap probability distribution in the prior week's forecast. If this distribution closely resembles the uniform distribution (the orange line), then we would say that our forecast closely resembles the generating distribution. In this example, we note that the observed distribution is very close to the theoretical distribution, indicating that our model did not have a consistent tendency to over- or under-estimate weekly hospitalizations and estimates of variance appear to be well-calibrated in aggregate.

eAppendix Figure 10: Histogram of Weekly MAPE (%) (Excluding March 31st)

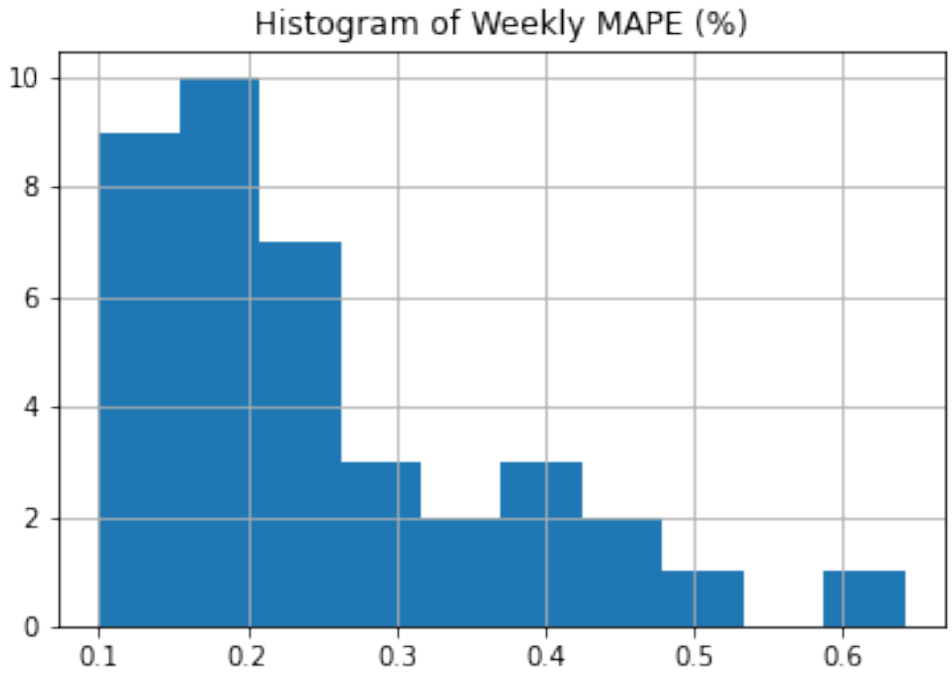

eAppendix Figure 10 displays a histogram of our realized MAPE from each week as compared to the prior week's forecast distribution of cumulative hospitalizations. Note that we exclude the forecast dated March 31st, 2020 because it skews the scale of the histogram. For the remaining forecast dates, we calculate the MAPE as the mean absolute error of cumulative hospitalizations over all forecast simulations for the week. Calculated this way, MAPE was less than 20% in 18 of the 39 forecast weeks and less than 50% in 37 of those weeks.

eAppendix Figure 11: Weekly Forecast of Cumulative Hospital Admissions, April 2020

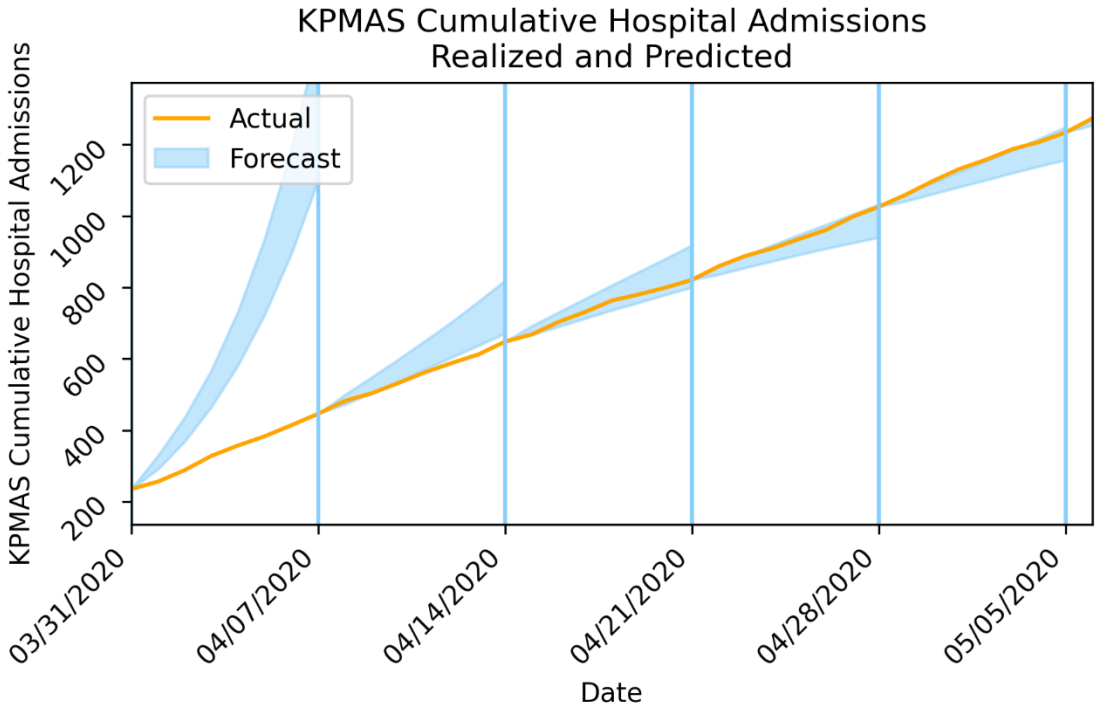

eAppendix Figure 11 displays the actual (orange) and forecast 95% Credible Interval (blue) of cumulative Hospital Admissions for the month of April 2020. Note that forecasts for the first two weeks predicted significantly more hospital admissions than were realized; however, the forecast quality increased significantly by the third week.

eAppendix Figure 12: Weekly Forecast of Cumulative Hospital Admissions, May 2020

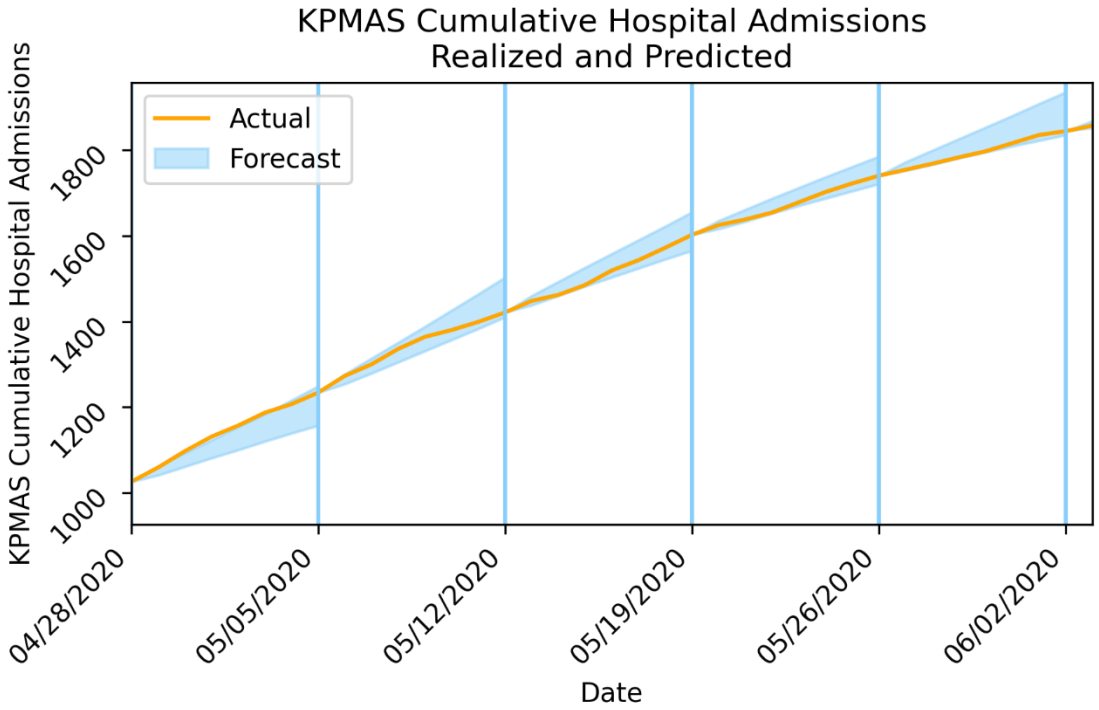

eAppendix Figure 12 displays the actual (orange) and forecast 95% Credible Interval (blue) of cumulative Hospital Admissions for the month of May 2020.

eAppendix Figure 13: Weekly Forecast of Cumulative Hospital Admissions, June 2020

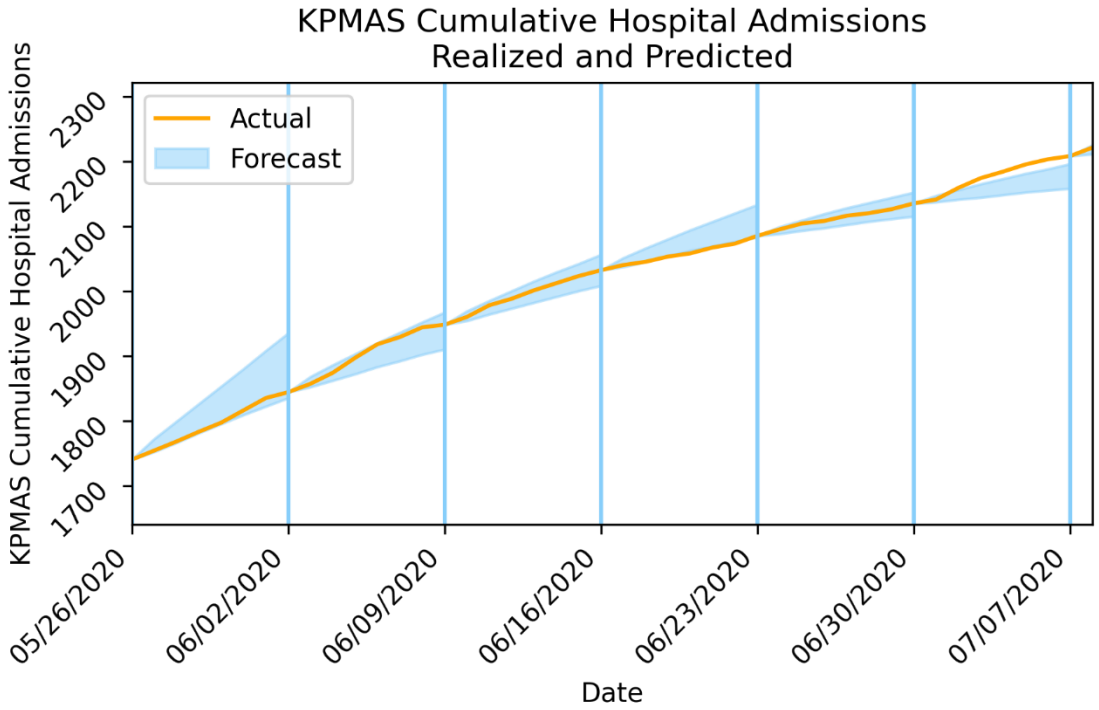

eAppendix Figure 13 displays the actual (orange) and forecast 95% Credible Interval (blue) of cumulative Hospital Admissions for the month of June 2020. Hospital admissions tapered during the beginning of the month, but they experienced an unexpected uptick at the beginning of July (the final week in this period).

eAppendix Figure 14: Weekly Forecast of Cumulative Hospital Admissions, July 2020

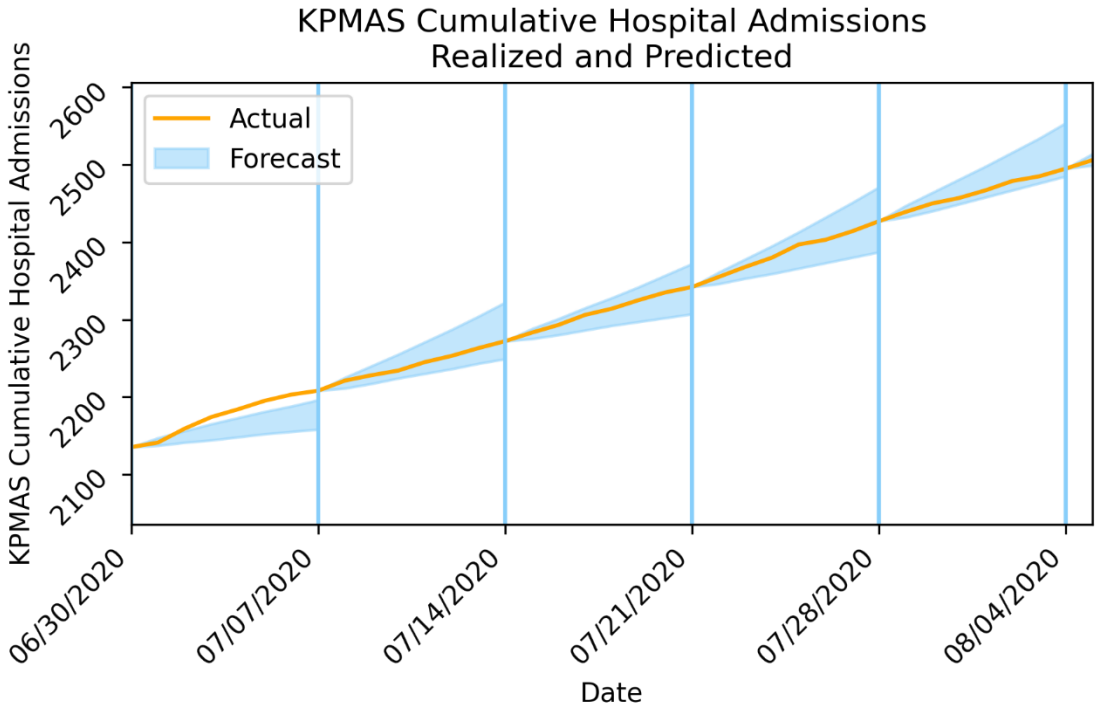

eAppendix Figure 14 displays the actual (orange) and forecast 95% Credible Interval (blue) of cumulative Hospital Admissions for the month of July 2020. Hospital admissions experienced a significant and unexpected uptick at the beginning of the month; however, the model was able to adapt quickly, and hospital admissions landed within the credible interval during future weeks.

eAppendix Figure 15: Weekly Forecast of Cumulative Hospital Admissions, August 2020

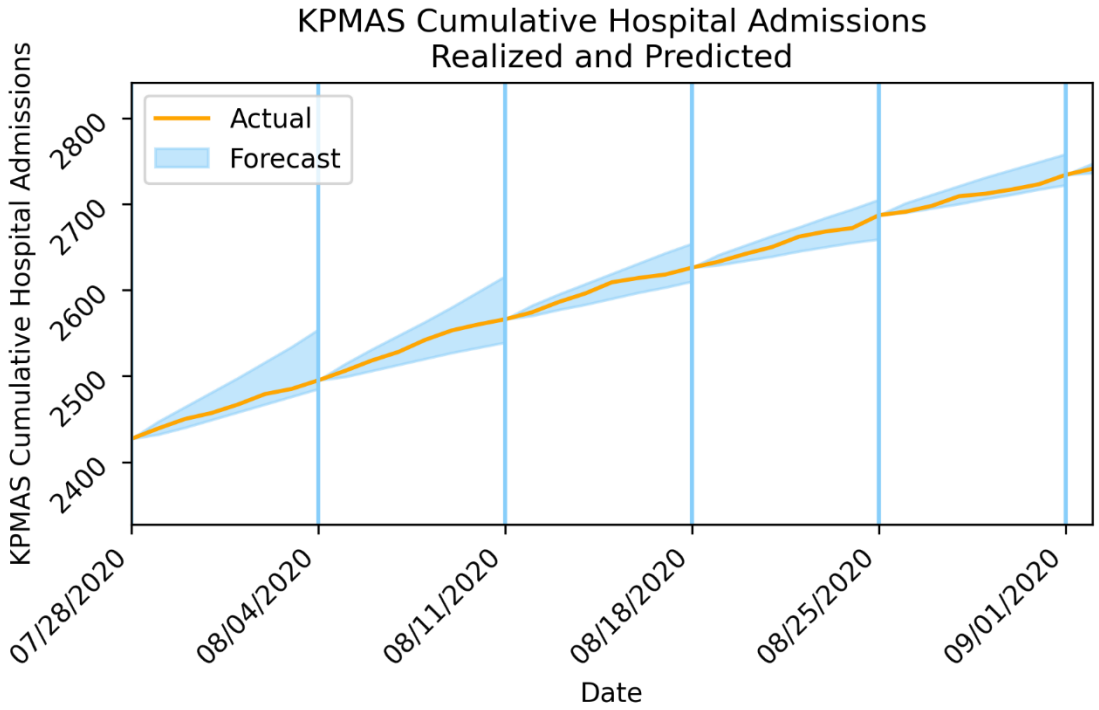

eAppendix Figure 15 displays the actual (orange) and forecast 95% Credible Interval (blue) of cumulative Hospital Admissions for the month of August 2020. Hospital admissions slowed during this period and the model's Credible Interval decreased in size, indicating greater confidence.

eAppendix Figure 16: Weekly Forecast of Cumulative Hospital Admissions, September 2020

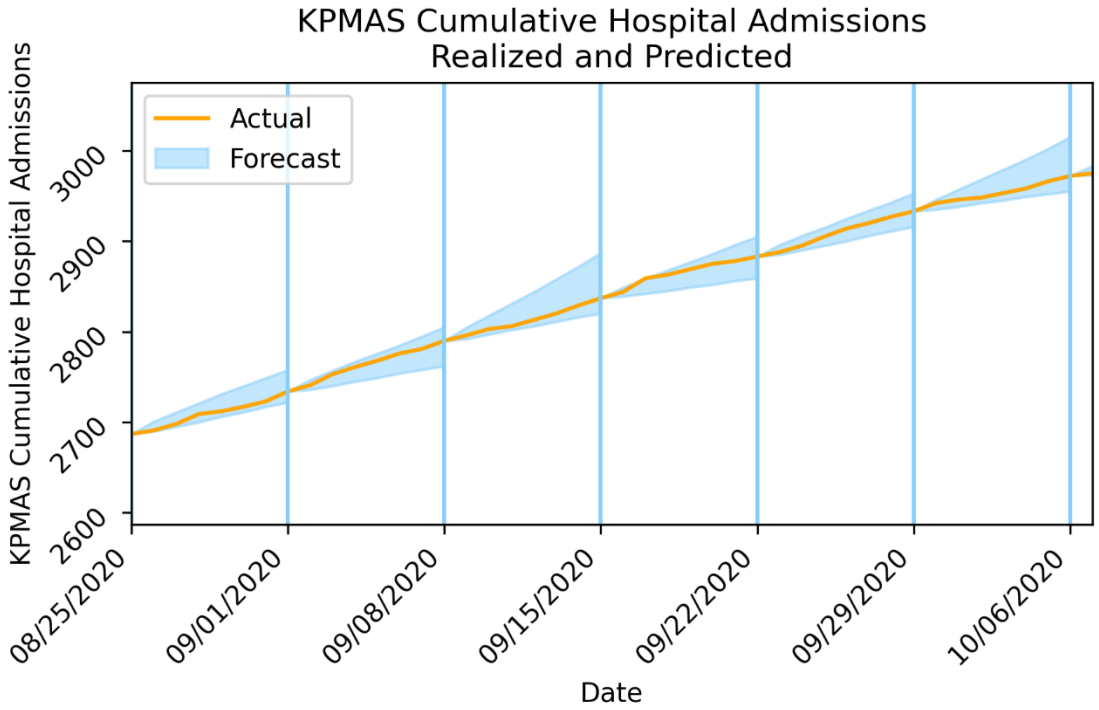

eAppendix Figure 16 displays the actual (orange) and forecast 95% Credible Interval (blue) of cumulative Hospital Admissions for the month of September 2020. There were no significant changes in system dynamics during this period relative to the prior month.

eAppendix Figure 17: Weekly Forecast of Cumulative Hospital Admissions, October 2020

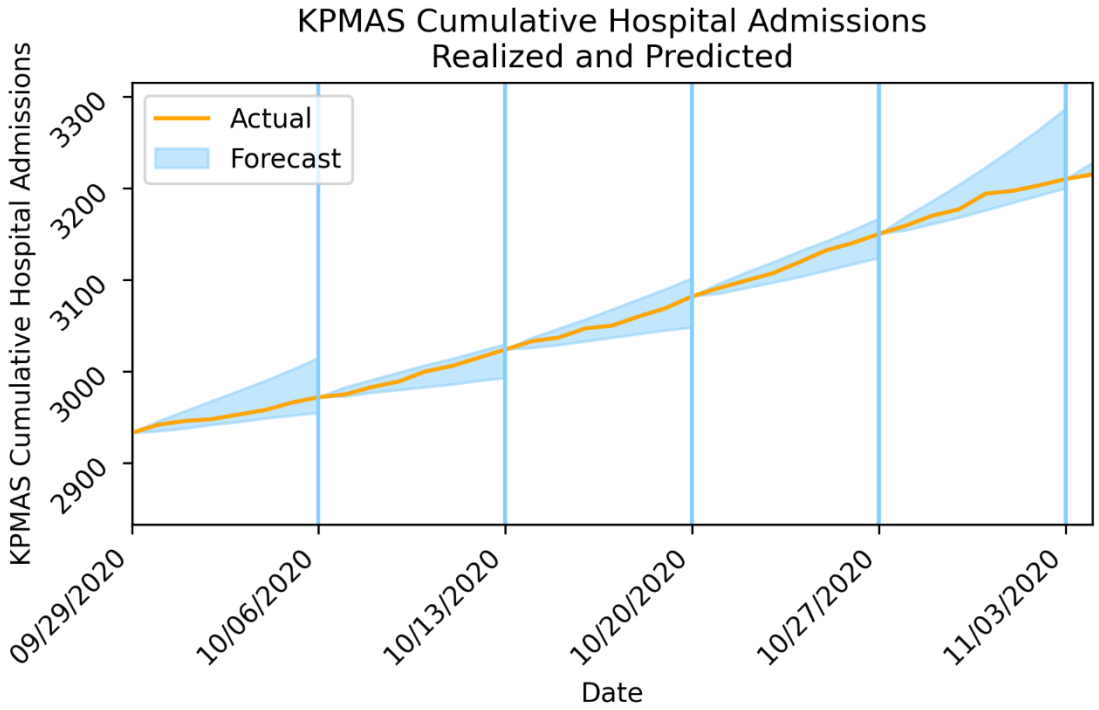

eAppendix Figure 17 displays the actual (orange) and forecast 95% Credible Interval (blue) of cumulative Hospital Admissions for the month of October 2020. Hospital admissions slowly began to increase in volume over the course of the month and the model kept pace with these increases.

eAppendix Figure 18: Weekly Forecast of Cumulative Hospital Admissions, November 2020

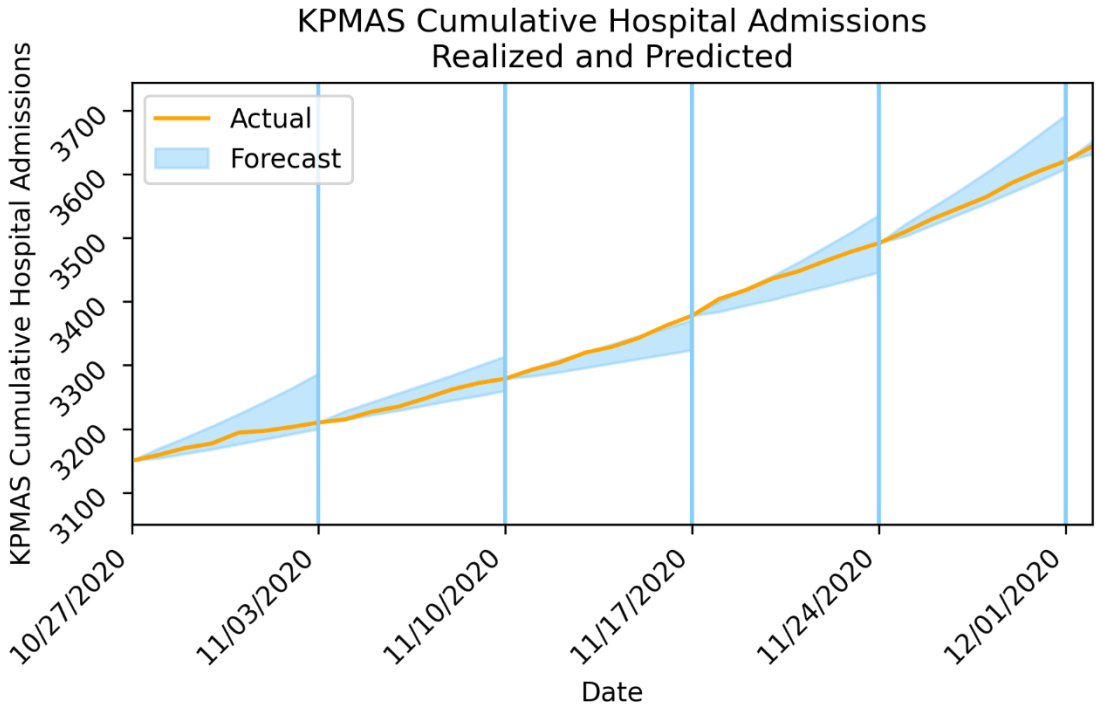

eAppendix Figure 18 displays the actual (orange) and forecast 95% Credible Interval (blue) of cumulative Hospital Admissions for the month of November 2020. This Figure captures the most significant uptick in hospital admissions during the Winter 2020 surge. Weekly forecasts displayed some uncertainty as to the magnitude of the surge, but realized admissions remained within expected bounds overall.

eAppendix Figure 19: Weekly Forecast of Cumulative Hospital Admissions, December 2020

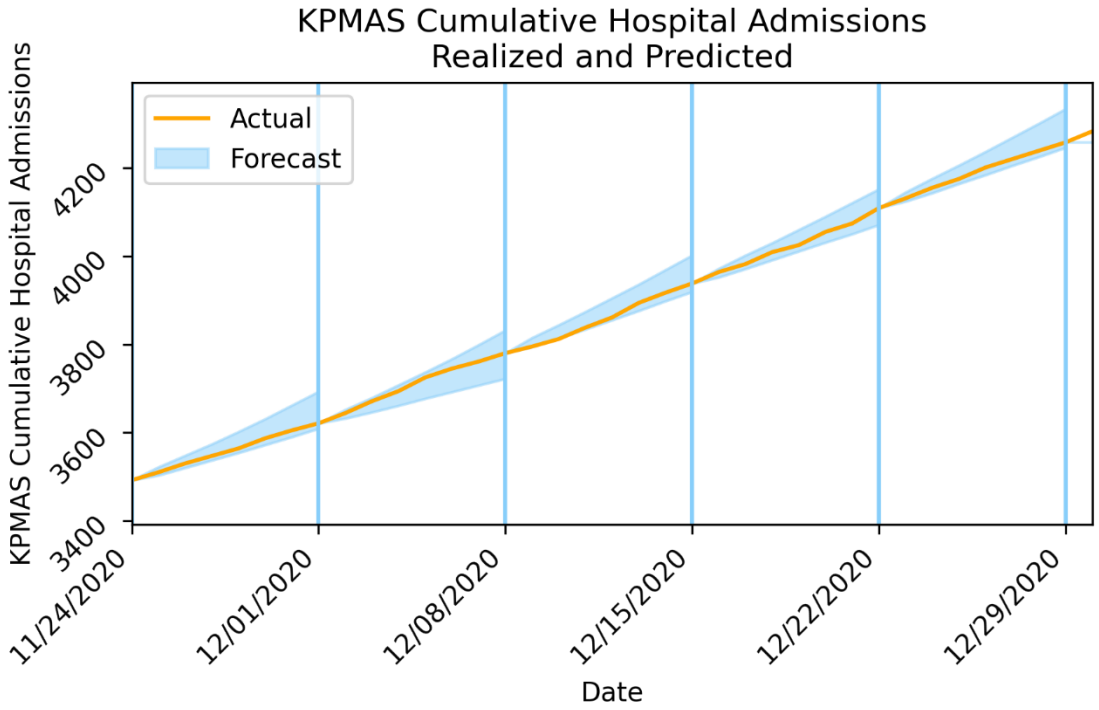

eAppendix Figure 19 displays the actual (orange) and forecast 95% Credible Interval (blue) of cumulative Hospital Admissions for the month of December 2020. Admissions accelerated during this month but remained within forecast limits.

eAppendix Table 1: XXXXX Population by Race

Race	**Share of XXXXX Population (%)**	**Share of SARS-CoV-2 Hospital Admissions (%)**
Black/African American	36.3	48.9
Hispanic/Latino	11.7	21.7
White	27.2	18.4
Other/Unknown	24.8	11.0

eAppendix Table 1 describes the share of hospital admissions experienced by different racial communities in the XXXXX region in comparison to the size of these communities. We found that the African American and Hispanic communities experienced significantly higher hospital admissions due to SARS-CoV-2 than did the White community, relative to the communities' respective sizes. This tendency reflects a national trend for SARS-CoV-2 to have an outsized impact on underprivileged communities.

eAppendix Table 2: Weekly Estimate of Most Recent Effective Reproductive Rate

Forecast Date	**Modeled Effective Reproductive Rate**
3/31/2020	3.078221
4/7/2020	1.208857
4/14/2020	0.860239
4/21/2020	0.760732
4/28/2020	0.897348
5/5/2020	1.084143
5/12/2020	0.942217
5/19/2020	0.817318
5/26/2020	0.8703
6/2/2020	0.749999
6/9/2020	0.782632
6/16/2020	0.828729
6/23/2020	0.678058
6/30/2020	0.737748
7/7/2020	1.073609
7/14/2020	1.038559
7/21/2020	1.065016
7/28/2020	1.115466
8/4/2020	0.977562
8/11/2020	0.903047
8/18/2020	0.844067
8/25/2020	0.87115
9/1/2020	0.888358
9/8/2020	0.990041
9/15/2020	0.901216
9/22/2020	0.996268
9/29/2020	0.935294
10/6/2020	0.86775
10/13/2020	0.991077
10/20/2020	1.147826
10/27/2020	1.188287
11/3/2020	1.070405
11/10/2020	0.960245
11/17/2020	1.174237
11/24/2020	1.298769
12/1/2020	1.102536
12/8/2020	1.133221
12/15/2020	1.035665
12/22/2020	1.033415

eAppendix Table 2 displays the model's estimate of the active effective reproductive rate for each forecast date in the study period. Note that this rate is only above 1.0 consistently during the initial outbreak of the pandemic, during July (the 'second wave') and during the final two months of 2020 (the 'third wave'). Even then, the effective reproductive rate is frequently still controlled (the maximum after the first week is only 1.3), indicating that social distancing and other control measures were likely quite effective at keeping the rate of spread relatively low compared to the uncontrolled rate observed before the implementation of any social distancing measures (in March, 2020).